Environ Monit Assess (2020) 192: 654
https://doi.org/10.1007/s10661-020-08588-5

Fire foci dynamics and their relationship with socioenvironmental factors and meteorological systems in the state of Alagoas, Northeast Brazil

José Francisco de Oliveira-Júnior · Washington Luiz Félix Correia Filho · Laurízio Emanuel Ribeiro Alves · Gustavo Bastos Lyra · Givanildo de Gois · Carlos Antonio da Silva Junior · Paulo José dos Santos · Bruno Serafini Sobral

Received: 27 October 2019 / Accepted: 31 August 2020 / Published online: 23 September 2020
© Springer Nature Switzerland AG 2020

Abstract The objective is to evaluate the fire foci dynamics via environmental satellites and their relationship with socioenvironmental factors and meteorological systems in the state of Alagoas, Brazil. Data considered the period between 2000 and 2017 and was obtained from CPTEC/INPE. Annual and monthly analyzes were performed based on descriptive, exploratory (boxplot) and multivariate statistics analyzes (cluster analysis (CA), principal component analysis (PCA)) and Poisson regression models (based on 2000 and 2010 census data). CA based on the Ward method identified five fire foci homogeneous groups (G_1 to G_5), while *Coruripe* did not classify within any group (NA); therefore, the CA technique was consistent (CCC = 0.772). Group G_1 is found in all regions of Alagoas, while G_2, G_5, and NA groups are found in *Baixo São Francisco, Litoral*, and *Zona da Mata* regions. Most fire foci were observed in the *Litoral* region. Seasonally, the largest records were from October to December months for all groups, influenced by the sugarcane harvesting period. The G4 group and *Coruripe* accounted for 60,767 foci (32.1%). The highest number of fire foci occurred in 2012 and 2015 (between 8000 and 9000 foci), caused by the action of the El Niño–Southern Oscillation. The Poisson regression showed that the dynamics of fire foci are directly associated with the Gini index and Human Development Index (models 1 and 3). Based on the PCA, the three components captured 78.8% of the total variance explained, and they were strongly influenced by the variables: population, GDP, and demographic density. The municipality of Maceió has the largest contribution from the fire foci, with values higher than 40%, and in PC1 and PC2 are related to urban densification and population growth.

Keywords Crop production · Environmental satellites · Multivariate analysis

J. F. de Oliveira-Júnior · W. L. F. C. Filho · P. J. dos Santos
Institute of Atmospheric Sciences (ICAT), Federal University of Alagoas (UFAL), Maceió, Alagoas 57072-260, Brazil

J. F. de Oliveira-Júnior · G. B. Lyra · B. S. Sobral
Postgraduate Program in Biosystems Engineering (PGEB), Federal Fluminense University (UFF), Niterói, Rio de Janeiro 24220-900, Brazil

L. E. R. Alves
National Institute for Space Research (INPE), Av. dos Astronautas, 1758-Jardim da Granja, São José dos Campos, São Paulo 12227-010, Brazil

G. B. Lyra
Department of Environmental Sciences (DCA), Institute of Forests (IF), Rural Federal University of Rio de Janeiro (UFRRJ), Seropédica, Rio de Janeiro 23897-000, Brazil

G. de Gois
School of Industrial Metallurgical Engineering of Volta Redonda, Technological Center, Federal Fluminense University (UFF), Volta Redonda, Rio de Janeiro 27255-250, Brazil

C. A. da Silva Junior (✉)
Department of Geography, State University of Mato Grosso (UNEMAT), Sinop, Mato Grosso 78550-000, Brazil
e-mail: carlosjr@unemat.br

B. S. Sobral
Land and Cartography Institute of Rio de Janeiro (ITERJ), State Secretary for the Environment and Sustentability (SEAS-RJ), Rua Regente Feijó, 7, Centro, Rio de Janeiro 20060-060, Brazil

Introduction

In recent decades, society and government entities have been mobilized in an integrated manner to minimize the effects of population vulnerability to the severity of extreme events across the globe, to which part is attributed to climate change (Stephenson et al. 2008; Forino et al. 2015; Trenberth et al. 2015). An example of these extremes are forest fires of anthropic origin and, generally, weather conditions (air temperature, rainfall, wind speed, relative humidity) and environmental conditions (vegetation, relief) in combination contribute to their behavior and spread (Chuvieco et al. 2012; Forino et al. 2015; Lima et al. 2020).

Forest fire occurrence interferes on composition and structure of vegetation in any location (Flanningan et al. 2000) with direct effects on the extinction of species of fauna and flora (Clemente et al. 2017; Oliveira-Júnior et al. 2017) and health risk to the population (Ribeiro 2008). In addition, the loss of vegetation cover via burning or forest fires results in increased greenhouse gas (GHG) emissions into the atmosphere, especially considering the carbon dioxide (CO_2), carbon monoxide (CO), nitrous oxide (N_2O), methane (CH_4), and ozone (O_3) emissions. These GHG reach several Metropolitan regions (MR) in Brazil (Silva de Souza et al. 2012; Mollmann Júnior et al. 2015; Zeri et al. 2016), influencing the biogeochemical cycles (Flanningan et al. 2000; Justino et al. 2010), and also stimulate environmental degradation (Brando et al. 2014; Jiang et al. 2014; Oliveira-Júnior et al. 2020).

In Brazil, the occurrences of fires are associated with the secular practices of fire use for tillage of large areas for the expansion of agricultural practices, mainly in the Central–West, Northeast, and North regions of the country (Alencar et al. 2004; Caúla et al. 2015; Bem et al. 2018; Lima et al. 2020; Oliveira-Júnior et al. 2020). The practice of burning is common in agricultural management (Clemente et al. 2017) and was intensified during the implementation of the National Alcohol Program (PROALCOOL), whose purpose was encouraging the expansion of sugarcane crop in the country, which began in 1975. PROALCOOL contributed to the increase in the burning of Brazilian sugarcane fields, since the burning of sugarcane straw as a method of eliminating unwanted vegetation in crop areas is also a common practice, especially in the state of Alagoas (SoA) (Mollmann Júnior et al. 2015). Due to environmental problems related mainly to the emission of pollutants released during the burning of the harvest sugarcane, the Brazilian Federal Government sanctioned, in 1998, the Law 2661 which involves the reduction of fire foci in sugarcane fields. In 2013, the state of Alagoas also sanctioned State Law No. 7454, which reiterates the same guidelines as the Federal Law, for the gradual elimination of fire usage in agricultural practices.

However, after the creation and modernization of laws and agricultural machinery, both were not sufficient to address the environmental impacts resulting from the significant increase in burnings and forest fires on biomes (Alencar et al. 2004; Brando et al. 2014; Caúla et al. 2015; Bem et al. 2018; Eugenio et al. 2019; Lima et al. 2020; Oliveira-Júnior et al. 2020).

In order to obtain real-time information and detect forest fires on a continental scale, the Brazilian National Institute for Space Research (INPE) monitors, through environmental satellites, the biomes, conservation units, and environmental protection areas (APAs) (Caúla et al. 2016; Oliveira-Júnior et al. 2017). The monitoring of fire foci is aimed at controlling areas susceptible to forest fires in Brazil and South America (SA) (CPTEC 2018). This detection of vegetation fires occurs from orbital sensors coupled to the following orbital platforms (satellites): NOAA (versions 15, 18, and 19); EUMETSAT (METOP-B), NASA (TERRA and AQUA), NPP (versions 375 and SUOMI), and GOES (versions 13 and 16), which operate in the 4-μm thermal range and then processed and stored in the Brazilian and SA data bank (BDQueimadas) (CPTEC 2018).

After the identification and detection of fire foci, several statistical methods have been used in order to assess patterns of spatial and temporal variability, and the intensity of these events, for example, cluster analysis (CA) (Caúla et al. 2015; Oliveira-Júnior et al. 2020), principal component analysis (PCA) (Rasilla et al. 2010; Paschalidou and Kassomenos 2016), artificial neural network (ANN), and logistic regression in a joint manner (Lall and Mathibela 2016; Bem et al. 2018). Caúla et al. (2015) used CA to identify the fire foci behavior in Brazil for 1988–2011 period and detected three fire foci homogeneous groups, where homogeneous group 1 (G_1) represented by only one region, the Northeastern Brazil. This group is influenced by meteorological systems and human activities, being the last a characteristic of most coastal cities along the Brazilian shoreline.

When considering this topic for SoA, the studies are scarce (Fernandes and Correia Filho 2013; Mollmann Júnior et al. 2015), and the existing ones do not relate to meteorological systems or land use and occupation. According to Caúla et al. (2015), during the years 2000 and 2015, the SoA is classified in the 10th place considering the total and density of fire foci per unit area (foci.km^{-2}).

Despite being one of the smallest Brazilian states, Caúla et al. (2015) showed that SoA presents great representativeness in the recording fire foci, which is due to its economy being based on the primary sector (agriculture and livestock), where sugarcane processing (sugar and ethanol) is the main economic vector in SoA (IBGE, 2018). Even in the face of this agricultural potential, the Human Development Index (HDI) indicates that Alagoas is one of the poorest states in Brazil (Malik 2013; Lyra et al. 2017). State revenues are strongly influenced by anomalies in climatic conditions. In this sense, studies seeking to characterize trends of drought (Lyra et al. 2017), strong rains (Lyra et al. 2014), or any other extreme climatic event in SoA, such as the occurrence of forest burning and fires, are justified. Therefore, the objective is to evaluate fire foci dynamics via environmental satellites and their relationship with anthropic (socioeconomic and land use) and environmental factors, as well as meteorological systems in the SoA.

Material and methods

Study area

The SoA is located in the eastern part (E) of the Brazilian Northeast Region, between latitudes 08° 48′ 05″ and 10° 30′ 09″ S and longitudes 35° 09′ 09″ and 38° 15′ 54″ W, with altitudes lower than 850 m mean above sea level (m.a.s.l.). The state borders northwest (NW) and west (W) with the states of Pernambuco, to the south the states of Sergipe and Bahia and the Atlantic Ocean to the east (E). The state is divided geopolitically in 102 municipalities, which compose six physiographic regions: *Zona da Mata*, *Litoral*, *Sertão*, *Sertão do São Francisco*, *Baixo São Francisco*, and Agreste (Fig. 1).

The SoA presents high annual rainfall variability, mainly in the E to W direction, with annual totals between 400 mm year^{-1} (*Sertão*) and 2000 mm year^{-1} (*Litoral*) (Molion and Bernardo 2002; Barros et al. 2012, Lyra et al. 2014). Regarding air temperature, the regions in the extreme N of the state register average values below 24 °C, due to the influence of the terrain—Plateau of *Borborema*. The highest temperatures are observed in the borderline of *Sertão* and *Baixo São Francisco* (BSF) regions, between the municipalities of *Delmiro Gouveia* and *Penedo*. In addition, higher temperatures, around 33 to 37 °C, occur during January and February months, while milder temperatures, around 27 to 32 °C, occur mainly in June and July months during the winter season (Lyra et al. 2011).

Meteorological systems in Alagoas, eastern Northeast Brazil

The SoA, located in the eastern Northeast of Brazil (ENEB), presents great spatial and temporal rainfall variability due to its orography, proximity to the coastal environment, and interaction of several mesoscale and synoptic meteorological systems over the region (Oliveira Júnior et al. 2012; Lyra et al. 2014). Also interacting upon this region are well-known climatic variability modes such as El Niño–Southern Oscillation (ENSO), Decadal Pacific Oscillation (DPO), and interhemispheric gradient of sea surface temperature (IGSST) of the Atlantic Ocean (Molion and Bernardo 2002; Kayano and Andreoli 2006; Kayano et al. 2013; Kayano and Capistrano 2014; Lyra et al. 2017; Correia Filho et al. 2019a).

Generally, rainfall in the SoA is influenced by meteorological systems at various scales such as trade winds, the Inter-Tropical Convergence Zone (ITCZ), the eastern disturbances waves (EDW) and frontal systems (FS) in the final cycle, upper tropospheric cyclonic vortex (UTCV), squall lines (SL), mesoscale convective systems (MCS), and sea–land breeze circulations (Moura and Shukla 1981; Harzallah et al. 1996; Molion and Bernardo 2002; Gois et al. 2005; Kouadio et al. 2012; Silva et al. 2011; Oliveira Júnior et al. 2012; Lyra et al. 2014; Correia Filho et al. 2016; Lyra et al. 2017; Silva 2017). Several of these systems are affected by modes of climatic variability such as ENSO, PDO, and IGSST (Lyra et al. 2017; Correia Filho et al. 2019a). In addition to the previously mentioned modes, the region is also affected by interseasonal modes, such as Madden-Julian Oscillation (MJO) (Souza et al. 2005), which takes place over the state usually in the months of February and May.

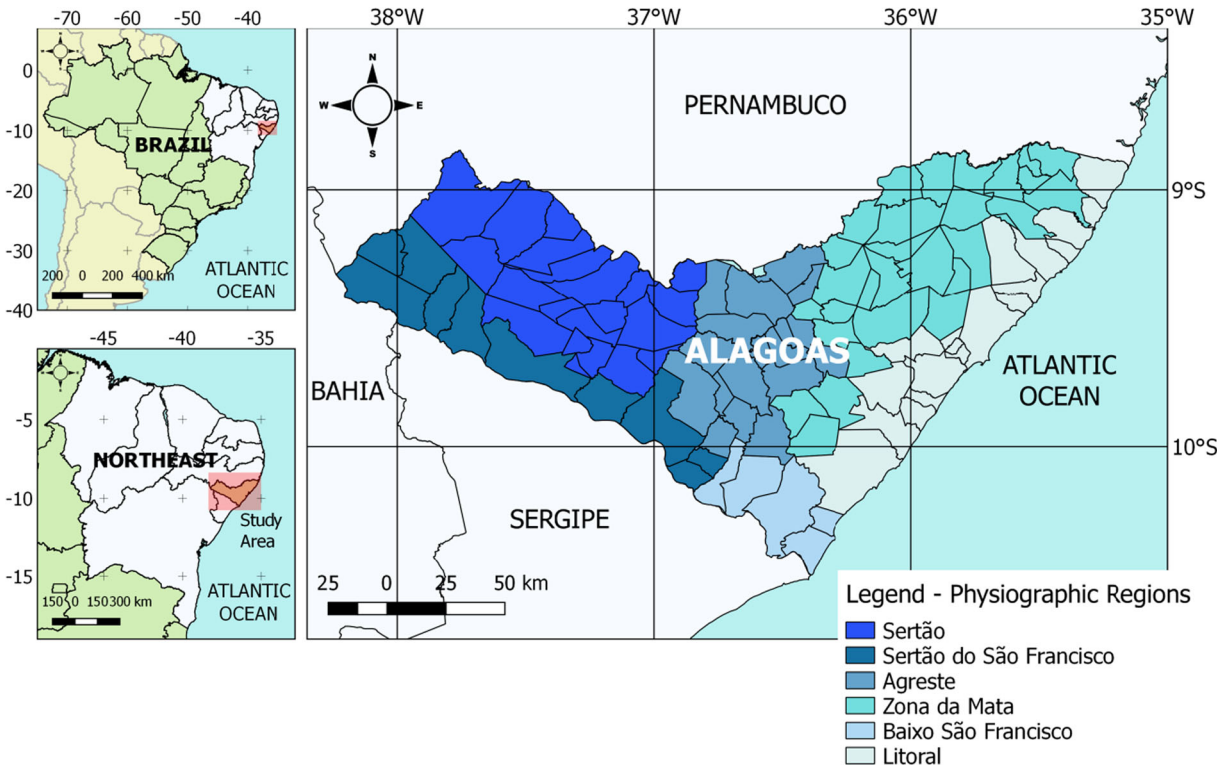

Fig. 1 The study region, highlighting Brazil (upper left corner), the Northeast region (lower left corner), and the SoA and its six physiographic regions (upper right corner)

Fire foci time series

The study was performed in a structured and sequenced manner, as shown in Fig. 2. The structure is subdivided into three stages: (i) obtaining and storing the different databases, (ii) applying the statistical methods, and (iii) analyzing and interpreting the results based on the thematic maps.

Fire foci database came from BDQueimadas, provided by Brazilian Center for Weather Forecasting and Climate Studies (CPTEC) and Brazilian Space Research Institute (INPE), were used and are made available at <http://queimadas.dgi.inpe.br/queimadas/bdqueimadas/>. These records were obtained from images of the following orbital sensors: (i) AVHRR version 3 (Advanced Very-High-Resolution Radiometer) from NOAA (versions 15, 18, and 19); version B of METOP-B (Meteorological Operation-B) and third generation of MSG (Meteosat Third Generation) from EUMETSAT; (ii) MODIS (Moderate Resolution Imaging Spectroradiometer) from NASA (TERRA and AQUA); (iii) VIIRS (Visible Infrared Imaging Radiometer Suite) from NPP (National Polar-orbiting Partnership) satellites of versions 375 and SUOMI; and (iv) images from GOES (Geostationary Operational Environmental Satellite) from NOAA (versions 13 and 16), which are processed and stored in the BDQueimadas database (CPTEC 2018). Based on fire foci data records, monthly time series were created for each of the 102 municipalities in the SoA between 2000 and 2017 years.

Multivariate and exploratory analysis

After the creation of monthly time series, the fire foci dynamics behavior was analyzed by two criteria: (i) composition of the annual and monthly fire foci totals, being submitted to the exploratory analysis (boxplot) in order to identify different periods and outliers, and (ii) evaluation of the fire foci time series behavior within the different homogeneous groups, using similar of fire foci patterns attained in CA.

The CA technique was applied to the fire foci time series using the R software version 3.1.1 (R Development Core Team 2017). Thus, the respective numbers of groups and dendrogram were determined. The number of groups adopted and the stratification of the stations were based on Ward's agglomerative

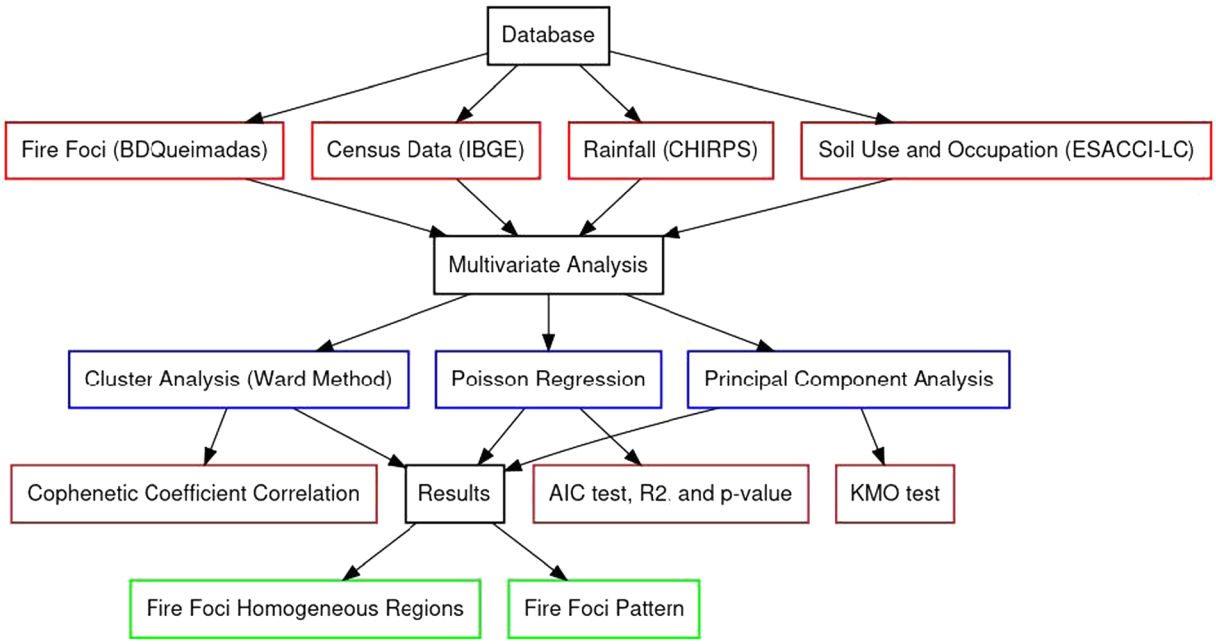

Fig. 2 Organization chart of the procedures carried out to obtain the fire foci patterns in SoA. The procedures are separated by rectangular boxes: the red ones to the database, the blue ones refer to the methodological procedure, the brown ones are the statistical tests inherent to the methods, and the green ones correspond to the exposure of the results of the respective methods

hierarchical method (Ward 1963) by Euclidean distance dissimilarity measure (Everitt and Dunn 1991). The Euclidean distance is given by Eq. 1:

$$d_E = \sqrt{\sum_{j=1}^{p}\left(x_{ik}-x_{kj}\right)^2} \quad (1)$$

where d_E = Euclidean distance and x_{ij} and x_{kj} = quantitative variables of p and k, respectively.

The Ward method (Ward 1963) is represented in Eq. 2 and consists on the distance between two groups being the squared sum of the two groups made on all the variables. In this method, dissimilarity is minimized, or the total sum of squared variables within groups is minimized, given by homogeneity within each group and heterogeneity outside each group (Lyra et al. 2014; Caúla et al. 2015).

$$W = \sum_{i=1}^{n} x_i^2 - \frac{1}{n}\sum\left(x_i\right)^2 \quad (2)$$

where W = inter-group homogeneity and heterogeneity through the sum of the squared deviations, n = number of analyzed values, and x_i = ith group element.

The degree of adjustment of the Ward method was assessed by cophenetic correlation coefficient (CCC). It measures the association between the dissimilarity matrix (F) and the matrix resulting from the simplification provided by clustering method (C). The CCC is based on Pearson coefficient correlation (r), being calculated between the dissimilarity matrix and the resulting matrix of the clustering process (Sokol and Rohlf 1962). Thus, the greater the value of r, the smaller will be the distortion. According to Valentin (2000), there is always a degree of distortion, since the r coefficient will never be equal to 1. However, Rohlf (1970) and Biagiotti et al. (2013) mentioned that the higher the value obtained for CCC, the smaller the distortion caused by CA. In practice, dendrograms with CCC < 0.7 indicate the inadequacy of the CA technique. The CCC is defined by Eq. 3.

$$\mathrm{CCC} = r_{\mathrm{cof}} = \frac{\sum_{j=1}^{n-1}\sum_{j'=j+1}^{n}\left(c_{jj'}-\overline{c}\right)\left(f_{jj'}-\overline{f}\right)}{\sqrt{\sum_{j=1}^{n-1}\sum_{j'=j+1}^{n}\left(c_{jj'}-\overline{c}\right)^2}\sqrt{\sum_{j=1}^{n-1}\sum_{j'=j+1}^{n}\left(f_{jj'}-\overline{f}\right)^2}} \quad (3)$$

where $\overline{c}$ and $\overline{f}$ are as arithmetic means defined by the Eqs. 4 and 5:

$$\overline{c} = \frac{\sum_{i=1}^{n} c_i}{n} \quad (4)$$

$$\overline{f} = \frac{\sum_{j=1}^{n} f_i}{n} \quad (5)$$

where CCC is the cophenetic correlation coefficient, c is the cophenetic matrix, $\overline{c}$ is the mean of the cophenetic matrix, f is the phenetic matrix, $\overline{f}$ is the mean of the phenetic matrix, and n is the number of elements.

Soil use and occupation

The fire foci analysis was based on annual thematic maps of the respective land use and land cover, from 2000 to 2015. The land use and cover data is derived from the European Space Agency - Climate Change Initiative - Land Cover (ESACCI-LC) (Bontemps et al. 2015; ESA 2018). The thematic maps correspond to version 2.0.7 of ESACCI-LC, with a spatial resolution of 300 × 300 m generated from SPOT-VEGETATION satellite data (1999 to 2012) and PROBA-V (2013–2015), available at the following address: <http://maps.elie.ucl.ac.be/CCI/viewer/download.php>.

Use of socioeconomic and environmental indicators

In addition to land use and coverage, data from socioeconomic indicators based on the 2000 and 2010 censuses, from the Brazilian Institute of Geography and Statistics (IBGE), were applied to the groups with the highest percentage of fire foci occurrence, which is formed by a smaller number of municipalities in groups G_2, G_4, and NA. Socioeconomic indicators used were total area (km^2), population size, demographic density (habitants km^{-2}), per capita income of municipalities, HDI, and Gini index (IBGE 2018a). Environmental data used were annual rainfall data from Climate Hazard Group InfRared Precipitation with Station (CHIRPS) (Funk et al. 2015; Paredes-Trejo et al. 2017), followed by harvested area and sugarcane production (IBGE 2018b), and land use and occupation (ESA 2018), from 2000 to 2010. All variables listed above were submitted to Poisson regression model and PCA.

Poisson regression models

In order to evaluate the interaction between fire foci and socioeconomic and environmental data, generalized linear models (GLM) were applied using Poisson regression. GLM is an extension of classical linear models developed by Nelder and Wedderburn (1972) to which three assumptions must be made: (i) the relationship between each explanatory variable and the response variable is approximately linear in its structure; (ii) residuals are independent with zero average and constant variance; and (iii) regression and residuals are not correlated.

GLM via Poisson regression were adapted for counting data in proportion or counting ratios forms, and their variables assume any positive integer value. The Poisson regression model has a positive mean and the logarithm of this value is the natural parameter of the Poisson distribution, where the logarithmic link is the canonical link for a GLM with random Poisson component, and $Y(\ln(\mu))$ the expected value for a Poisson variables Y and X is an explanatory variable. The log-linear model is based on Eq. 6:

$$\ln(\mu) = \alpha + \beta X \tag{6}$$

For this model, the mean satisfies the exponential relation according to Eq. 7:

$$\mu = \exp(\alpha + \beta X) = e^{\alpha+\beta X} \tag{7}$$

Using the regression results, all the models were evaluated based on the residual deviance and the Akaike information criterion (AIC) methods. Residual deviance is a measure of fit quality of the model, based on the comparison between the deviances of the proposed models (M_1) versus the complete or saturated (M_2) model, and the parameters of M_1 and M_2 are $p < n$ and $q < p$ degrees of freedom, respectively, (Eq. 8):

$$D_{\text{Res}} = \frac{D(M_1) - D(M_2)}{(p-q)} \tag{8}$$

The AIC test preselects a set of explanatory variables that interact with one another (Akaike 1974). The final composition of the model was performed in a multiple manner, with verification of association degree between the variables based on the significance level (p value < 0.10), and those that do not have interaction or multicollinearity were excluded, according to Eq. 9:

$$\text{AIC} = -2L + 2k \tag{9}$$

where L is the maximum of log-likelihood and k is the number of explanatory variables in the model. Lower AIC means that the model has a better fit.

From the regression analysis, four models were built based on the 2000 and 2010 censuses made available by IBGE (2018b). Model 1 (GLM1) consists of socioeconomic variables, being formed by Population size of the municipality, demographic density, total area of the municipality, HDI, Gini index, and per capita income.

Model 2 (GLM2) is composed of environmental variables (accumulated annual rainfall), sugarcane production (annual harvested area and production volume), and the percentage of land use and cover for agricultural cultivation. Model 3 (GLM3) was built on the junction of GLM1 and GLM2. Finally, model 4 (GLM4) is formed by the HDI only.

Principal component analysis

In the evaluation of fire foci in the SoA the factor analysis via PCA was also applied. PCA reduces the number of variables in a data set, thus preserving the total variance, and also identifies patterns and processes associated with the observed variables (Heinl et al. 2004; Moreno and Chuvieco 2013; Correia Filho and Silva Aragão 2014). The calculation of the factor loadings of the PCA is given by Eq. 10:

$$F_p = ej_1U_1 + ej_2U_2 + ej_3U_3 + \ldots + a_{nb}U_p \quad \text{or} \quad F_p = \sum_{i=1}^{p} e_{ip}U_p \tag{10}$$

where F_p is the original normalized matrix, e_p is the eigenvector, and U_1, U_2, …, U_b are the linear combinations between the eigenvector matrix and the observation matrix F.

In assessing the significance of the results of the PCA, the Kaiser–Meyer–Olkin (KMO) test was used, in which the significance ranges from 0 to 1. It is noteworthy that the test acts as a quality indicator of the database.

$$\mathrm{KMO} = \frac{\left(\sum_j \sum_{k \neq j} r_{jk}^2\right)}{\left(\sum_j \sum_{k \neq j} r_{jk}^2 + \sum_j \sum_{k \neq j} p_{jk}^2\right)} \tag{11}$$

where r is the standard correlation coefficient and p is the standard partial correlation coefficient.

According to Corrar et al. (2007), the KMO test values below 0.5 indicate that the matrix should be discarded, between 0.5 and 0.7 of the results are reasonable, between 0.7 and 0.9 are good, and above 0.9 is considered great.

To identify the ideal number of principal components (PC), the Kaiser method was used, which selects eigenvalues greater than 1 ($\lambda > 1$) (Hongyu et al. 2016). Besides the factorial load, the degree of influence of all PCs from their respective factorial load (scores) was also checked. All calculations used in the study were performed in the R version 3.4-1 environment software (R Development Core Team 2017).

Results and discussion

Fire foci homogeneous regions

The CA technique via the Ward method identified five fire foci homogeneous groups (G_1 to G_5) and one municipality (*Coruripe*) that do not form a group (NA) in Alagoas (Fig. 3a). Summing squares of homogeneity and intragroup heterogeneity deviations (W) indicated five clusters as ideal (Fig. 3b). The formation of fire foci homogeneous groups via CA technique presented consistency of 0.772. The standardized mean of Euclidean distance was adequate for fire foci data, with CCC > 0.70 as recommended by Rohlf (1970).

Based on multivariate analysis, the SoA showed a heterogeneous spatial distribution of fire foci (Fig. 4). In group 1 (G_1), with 78.9 ± 181.0 foci, consisting of 53 municipalities, corresponding to 10.4% (19,782 foci) of the total during the time series. It is worth mentioning that G_1 covered all the physiographic regions of the state, with emphasis on the *Agreste* region (Table 1). Group 2 (G_2) registered 137.1 ± 287.7 foci within four municipalities of the state, corresponding to 14.4% of foci (27,284). G_2 comprised only of *Zona da Mata* (ZM) and *Litoral* regions. Group 3 (G_3), with 197.7 ± 425 foci comprises of 12 municipalities, corresponding to 17.7% (33,382) of the total fire foci. G_3 encompassed only regions *Agreste*, BSF, *Litoral*, and ZM regions. Group 4 (G_4) registered 173.4 ± 403.4 foci in three municipalities, corresponding to 20.4% (38,614) of the total fire foci, followed by group 5 (G_5) with 186.2 ± 440.9 foci in the period, comprising 29 municipalities, and 25.4% (48,080) of the total fire foci. The municipality of *Coruripe*, which did not form a statistical group, belongs to the *Litoral* region, with 102.4 ± 193.4 foci, and comprises 11.7% of fire foci, with a total of 22,153 foci. Both G_3, G_4, and G_5 are the largest groups of fire foci formed in the SoA, while G_1 and G_2 are smaller (Table 2).

It is worth mentioning that the distribution and concentration of the homogeneous groups of minor fire foci were registered in the BSF, *Litoral*, and ZM regions. The largest groups are distributed throughout the SoA

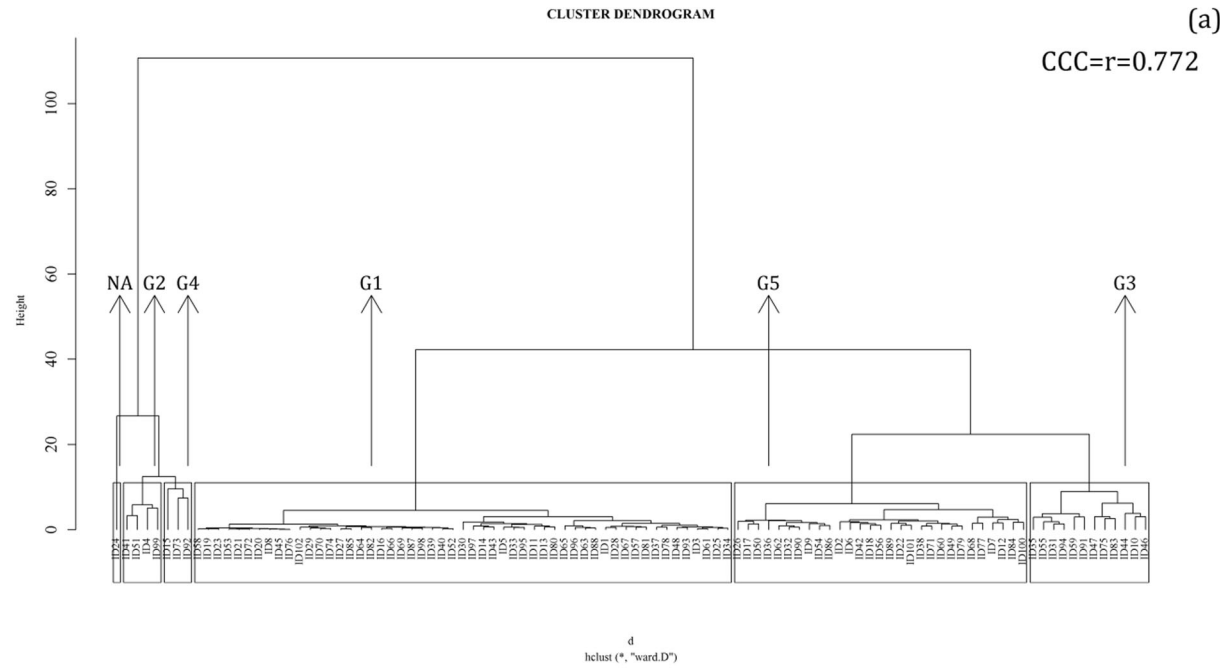

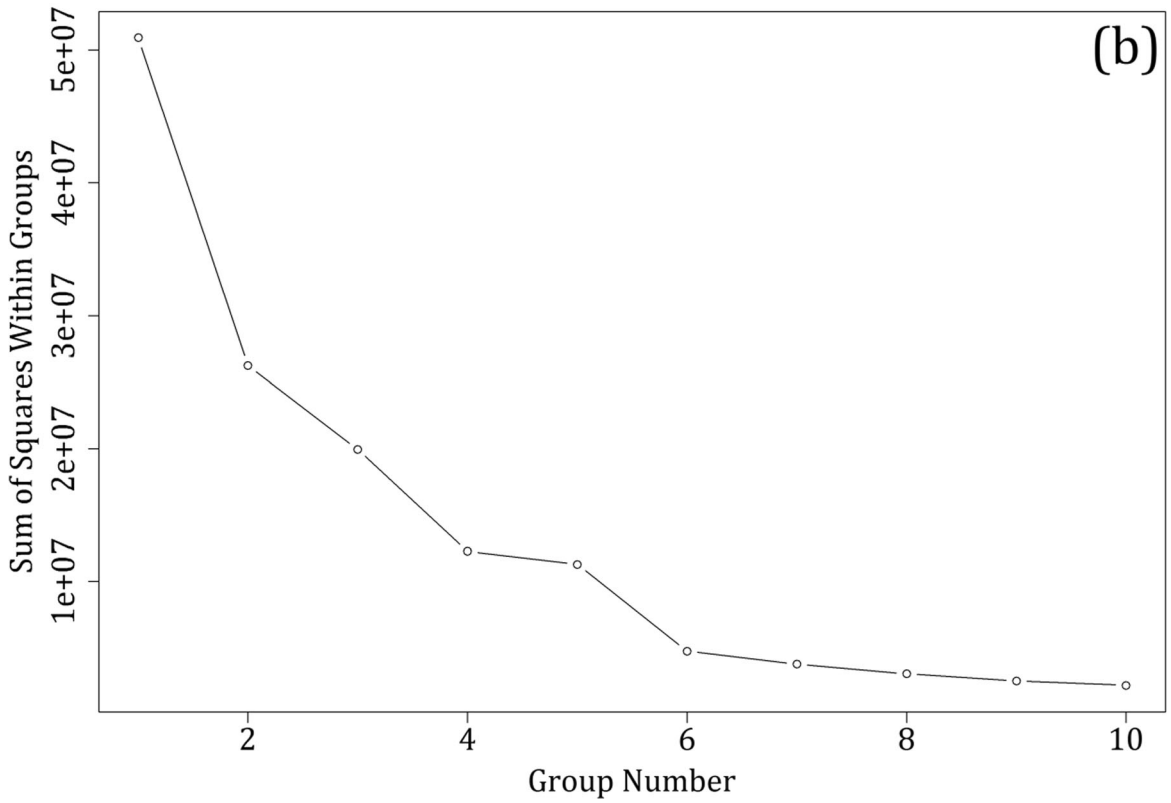

Fig. 3 Identification of the ideal number of homogeneous groups from the dendrogram (**a**) and the total of the quadratic sum within the groups, based on the fire foci time series in Alagoas (**b**). The CCC value credits the number of selected homogeneous groups

with emphasis on municipalities belonging to the *Litoral* region (Fig. 4). The *Litoral* region is the most populated region holding 42.4% (IBGE 2018a, b) of the state's population. It is also where the state's main economic activities—combination of sugarcane cultivation and sugar–alcohol industrial plants—take place (Fernandes and Correia Filho 2013; IBGE 2018a). The increase in fire foci is highest in municipalities that have sugarcane planting areas and sugar–alcohol mills (Clemente 2011; Belo and Santos 2013).

It is worrying that part of these records of fire foci occur in environmental preservation areas (APA) and conservation units (UC), and thus the fire foci correspond to the burning and fires and extend from the boundaries of the leased area to the planting of sugarcane and invade the protected areas, as reported by Melo (2011) when assessing the Zona da Mata Pernambucana. According to Melo (2011), only 0.72% of the remaining 7.0% of the Atlantic Forest is located in UC, and most of them are private properties, with sugar–alcohol activities. In some municipalities located in the Sertão Alagoano, such as Mata Grande, the occurrence of fire foci is due to the deforestation of the Caatinga for cleaning of the area for subsistence agriculture, as reported by Neves et al. (2018) and Santos Silva et al. (2019).

Fire foci occurred in all physiographic regions of Alagoas. However, this phenomenon is not continuous; there are areas with smaller (G_2 and G_4) and larger (G_1, G_3 and G_5) foci concentrations and, therefore, the greater territorial extension does not always represent a larger quantity of fire foci, similar to the result obtained by Pereira and Silva (2016) for the state of Paraíba, NEB (Table 3).

Although the highest foci occurrences were recorded in October, November, and December months, the fire foci monthly distribution was non-uniform, similar to the result obtained by Caúla et al. (2015). The lowest records were registered in the months corresponding to the transition and rainy seasons in the SoA (Oliveira Júnior et al. 2012; Lyra et al. 2014).

In the monthly series, quite a few outliers were registered, except for September and October months (Fig. 5a). Regarding outliers, some years of the time series registered higher occurrence, where heat foci is highly variable, especially in 2008, 2012, 2015, and 2016 (Fig. 5b). The fire foci annual distribution presents a high variability, especially the years highlighted

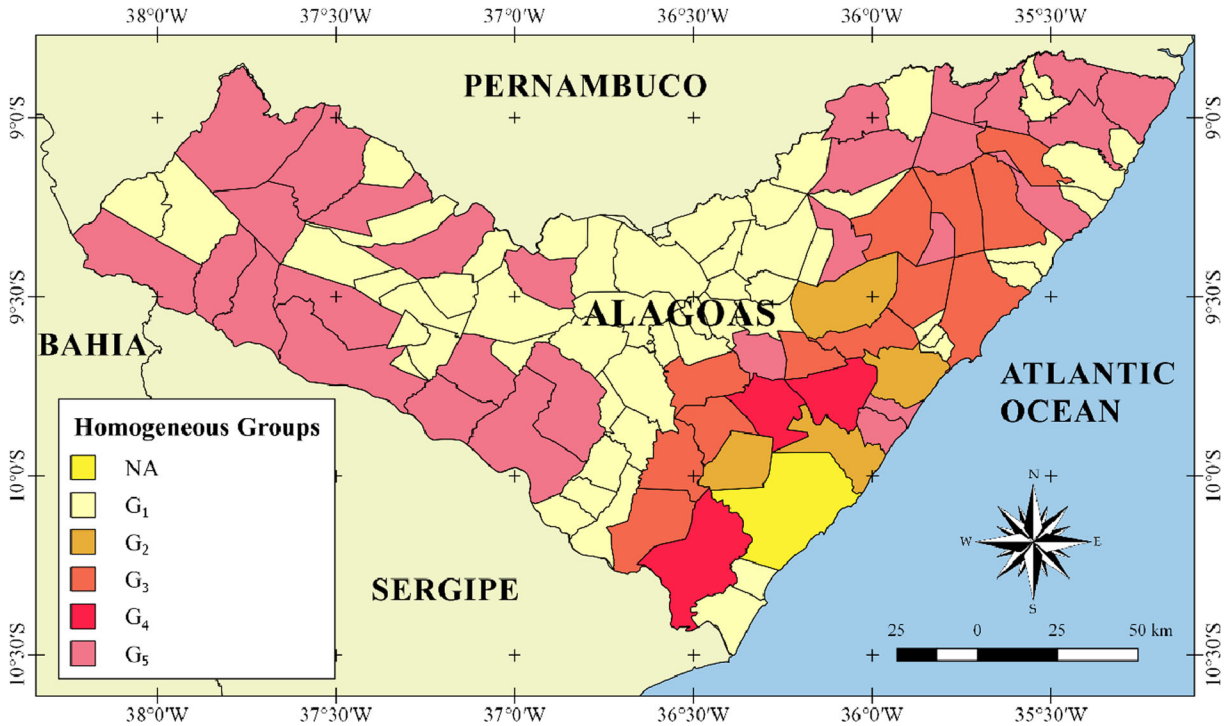

Fig. 4 Fire foci spatial distribution of the homogeneous groups (G_1 to G_5) and the municipality that did not form group (NA), in the state of Alagoas, for the period from 2000 to 2017

Table 1 Location of all 102 municipalities of Alagoas, Brazil, with its respective geographic coordinates and average altitude (m)

ID	Municipalities	Latitude (°)	Longitude (°)	Altitude (m)
1	Água Branca	09° 15′ 39″ S	37° 56′ 10″ W	570
2	Anadia	09° 41′ 04″ S	36° 18′ 15″ W	153
3	Arapiraca	09° 45′ 07″ S	36° 39′ 39″ W	264
4	Atalaia	09° 30′ 07″ S	36° 01′ 22″ W	54
5	Barra de Santo Antônio	09°24′18″ S	35° 30′ 25″ W	10
6	Barra de São Miguel	09° 50′ 24″ S	35° 54′ 28″ W	2
7	Batalha	09° 40′ 40″ S	37° 07′ 29″ W	120
8	Belém	09° 34′ 16″ S	36° 29′ 32″ W	311
9	Belo Monte	09° 49′ 42″ S	37° 16′ 48″ W	30
10	Boca da Mata	09° 38′ 29″ S	36° 13′ 13″ W	132
11	Branquinha	09° 14′ 44″ S	36° 00′ 55″ W	100
12	Cacimbinhas	09° 24′ 01″ S	36° 59′ 25″ W	270
13	Cajueiro	09° 23′ 48″ S	36° 09′ 13″ W	102
14	Campestre	08° 50′ 45″ S	35° 34′ 05″ W	0
15	Campo Alegre	09° 46′ 55″ S	36° 21′ 03″ W	176
16	Campo Grande	09° 57′ 28″ S	36° 47′ 30″ W	142
17	Canapi	09° 07′ 01″ S	37° 36′ 08″ W	342
18	Capela	09° 24′ 27″ S	36° 04′ 25″ W	84
19	Carneiros	09° 28′ 57″ S	37° 22′ 38″ W	347
20	Chã Preta	09° 15′ 19″ S	36° 17′ 46″ W	463
21	Coité do Nóia	09° 37′ 56″ S	36° 34′ 43″ W	280
22	Colônia Leopoldina	08° 54′ 32″ S	35° 43′ 30″ W	140
23	Coqueiro Seco	09° 38′ 18″ S	35° 48′ 11″ W	31
24	Coruripe	10° 07′ 32″ S	36° 10′ 32″ W	16
25	Craíbas	09° 37′ 05″ S	36° 46′ 05″ W	252
26	Delmiro Gouveia	09° 23′ 19″ S	37° 59′ 57″ W	256
27	Dois Riachos	09° 23′ 33″ S	37° 06′ 02″ W	245
28	Estrela de Alagoas	09° 23′ 25″ S	36° 45′ 36″ W	0
29	Feira Grande	09° 54′ 01″ S	36° 40′ 39″ W	220
30	Feliz Deserto	10° 17′ 31″ S	36° 18′ 22″ W	6
31	Flexeiras	09° 11′ 51″ S	35° 46′ 51″ W	78
32	Girau do Ponciano	09° 53′ 03″ S	36° 49′ 44″ W	244
33	Ibateguara	08° 58′ 21″ S	35° 56′ 22″ W	505
34	Igaci	09° 32′ 13″ S	36° 38′ 01″ W	240
35	Igreja Nova	10° 07′ 31″ S	36° 39′ 43″ W	14
36	Inhapi	09° 13′ 17″ S	37° 44′ 55″ W	410
37	Jacaré dos Homens	09° 38′ 08″ S	37° 12′ 17″ W	135
38	Jacuípe	08° 50′ 30″ S	35° 27′ 36″ W	74
39	Japaratinga	09° 05′ 18″ S	35° 15′ 30″ W	5
40	Jaramataia	09° 39′ 34″ S	37° 00′ 07″ W	164
41	Jequiá da Praia	10° 0′ 22″ S	36° 01′ 24″ W	5
42	Joaquim Gomes	09° 08′ 00″ S	35° 44′ 54″ W	104
43	Jundiá	08° 56′ 05″ S	35° 34′ 25″ W	94
44	Junqueiro	09° 55′ 31″ S	36° 28′ 33″ W	175
45	Lagoa da Canoa	09° 49′ 47″ S	36° 44′ 16″ W	283
46	Limoeiro de Anadia	09° 44′ 26″ S	36° 30′ 10″ W	140

Table 1 (continued)

ID	Municipalities	Latitude (°)	Longitude (°)	Altitude (m)
47	Maceió	09° 39′ 57″ S	35° 44′ 07″ W	16
48	Major Isidoro	09° 31′ 56″ S	36° 59′ 06″ W	182
49	Maragogi	09° 00′ 44″ S	35° 13′ 21″ W	5
50	Maravilha	09° 14′ 08″ S	37° 21′ 00″ W	362
51	Marechal Deodoro	09° 42′ 37″ S	35° 53′ 42″ W	31
52	Maribondo	09° 34′ 38″ S	36° 18′ 19″ W	157
53	Mar Vermelho	09° 26′ 51″ S	36° 23′ 17″ W	542
54	Mata Grande	09° 07′ 03″ S	37° 43′ 56″ W	633
55	Matriz de Camaragibe	09° 09′ 06″ S	35° 32′ 00″ W	16
56	Messias	09° 23′ 00″ S	35° 50′ 30″ W	148
57	Minador do Negrão	09° 18′ 19″ S	36° 51′ 53″ W	270
58	Monteiropólis	09° 36′ 10″ S	37° 14′ 54″ W	228
59	Murici	09° 18′ 24″ S	35° 56′ 36″ W	82
60	Novo Lino	08° 54′ 54″ S	35° 38′ 48″ W	146
61	Olho D'Água das Flores	09° 32′ 10″ S	37° 17′ 38″ W	286
62	Olho D'Água do Casado	09° 30′ 07″ S	37° 50′ 02″ W	230
63	Olho D'Água Grande	10° 03′ 30″ S	36° 49′ 00″ W	118
64	Olivença	09° 31′ 07″ S	37° 11′ 26″ W	231
65	Ouro Branco	09° 10′ 00″ S	37° 21′ 24″ W	380
66	Palestina	09° 40′ 19″ S	37° 19′ 45″ W	160
67	Palmeira dos Índios	09° 24′ 26″ S	36° 37′ 39″ W	342
68	Pão de Açúcar	09° 44′ 54″ S	37° 26′ 12″ W	19
69	Pariconha	09° 15′ 10″ S	38° 00′ 17″ W	0
70	Paripueira	09° 27′ 54″ S	35° 33′ 06″ W	0
71	Passo de Camaragibe	09° 14′ 18″ S	35° 29′ 36″ W	4
72	Paulo Jacinto	09° 21′ 58″ S	36° 22′ 11″ W	292
73	Penedo	10° 17′ 25″ S	36° 35′ 11″ W	27
74	Piaçabuçu	10° 24′ 20″ S	36° 26′ 04″ W	3
75	Pilar	09° 35′ 50″ S	35° 57′ 24″ W	13
76	Pindoba	09° 28′ 31″ S	36° 17′ 24″ W	310
77	Piranhas	09° 37′ 25″ S	37° 45′ 24″ W	88
78	Poço das Trincheiras	09° 18′ 45″ S	37° 17′ 08″ W	292
79	Porto Calvo	09° 02′ 42″ S	35° 23′ 54″ W	54
80	Porto de Pedras	09° 09′ 30″ S	35° 17′ 42″ W	22
81	Porto Real do Colégio	10° 11′ 09″ S	36° 50′ 24″ W	10
82	Quebrangulo	09° 19′ 08″ S	36° 28′ 16″ W	366
83	Rio Largo	09° 28′ 42″ S	35° 51′ 12″ W	39
84	Roteiro	09° 49′ 58″ S	35° 58′ 40″ W	32
85	Santa Luzia do Norte	09° 36′ 12″ S	35° 49′ 21″ W	32
86	Santana do Ipanema	09° 22′ 42″ S	37° 14′ 43″ W	250
87	Santana do Mundaú	09° 10′ 05″ S	36° 13′ 20″ W	221
88	São Brás	10° 07′ 40″ S	36° 54′ 02″ W	25
89	São José da Laje	09° 00′ 35″ S	36° 03′ 30″ W	256
90	São José da Tapera	09° 33′ 30″ S	37° 22′ 52″ W	255
91	São Luís do Quitunde	09° 19′ 06″ S	35° 33′ 40″ W	4
92	São Miguel dos Campos	09° 46′ 52″ S	36° 05′ 37″ W	12

Table 1 (continued)

ID	Municipalities	Latitude (°)	Longitude (°)	Altitude (m)
93	São Miguel dos Milagres	09° 15′ 56″ S	35° 22′ 23″ W	1
94	São Sebastião	09° 56′ 01″ S	36° 33′ 15″ W	201
95	Satuba	09° 33′ 48″ S	35° 49′ 28″ W	6
96	Senador Rui Palmeira	09° 27′ 59″ S	37° 27′ 25″ W	352
97	Tanque D'Arca	09° 31′ 55″ S	36° 25′ 58″ W	212
98	Taquarana	09° 38′ 42″ S	36° 29′ 50″ W	159
99	Teotônio Vilela	09° 54′ 19″ S	36° 21′ 10″ W	156
100	Traipu	09° 58′ 14″ S	37° 00′ 12″ W	10
101	União dos Palmares	09° 09′ 46″ S	36° 01′ 55″ W	155
102	Viçosa	09° 22′ 17″ S	36° 14′ 27″ W	210

above, due to the increase in the number of environmental satellites and improvement of the orbital sensors, notified by Caúla et al. (2016), Clemente et al. (2017) and Eugenio et al. (2019) (Fig. 5c).

In 2013, the reduction of fire foci occurrence is associated to decreasing on environmental satellites number and sugarcane production (harvested area). There has been a significant increase in fire foci in the years 2008, 2011/2012 (La Niña), and 2015/2016 (El Niño), all associated with the ENSO phases, respectively (Marengo et al. 2017a, b; Correia Filho et al. 2018; Correia Filho et al. 2019a). La Niña episodes had different characteristics, the year 2008 (2012) was characterized as a rainy (dry) year. Correia Filho et al. (2019a, b), when evaluating the rainfall on the Atlantic Forest Biome, found for 2008 (2012) an average monthly of 118.0 mm month^{-1}, an increase of 3.82% compared with climatology (decrease of 84.2 mm month^{-1}, a reduction of 25.91% compared with climatology). Both patterns between rainfall and drought configure the increase of the planting/crop area and the occurrence of drought periods resulting from vegetative stress and hence in increased fire foci (Barros Santiago et al. 2019; Correia Filho et al. 2019b).

Exploratory analysis of fire foci time series

Based on boxplot, the fire foci analysis in seasonal and annual scales registered by each homogeneous group were evaluated (Figs. 6 and 7). In general, all homogeneous groups recorded the higher fire foci occurrences between September and December months, followed by smallest records between April and August months, except G_4 that presented different period for the lower fire foci occurrence, from January to March months (Fig. 6d). This seasonal pattern found by G_4 presented similar characteristics, being verified by White and White (2017) in the state of Sergipe. However, with a lower record of 38,614 (G_4) foci against 2600 (total foci in the state of Sergipe, between the years 2000 and 2015). The period from September to December is associated with two factors: (i) the transition from rainy season to dry season (Lyra et al. 2014) and (ii) the

Table 2 Distribution of municipalities corresponding to the six homogeneous groups of fire foci in the SoA, with their totals, percentage (%), averages, and standard deviations in the period from 2000 to 2017

Fire foci homogeneous groups	Municipalities	Percentage (%) and total (foci)	Average and standard deviation
G_1	53	10.4% and 19,782	78.9 ± 181.0
G_2	4	14.4% and 27,284	137.1 ± 287.7
G_3	12	17.7% and 33,382	197.7 ± 425.8
G_4	3	20.4% and 38,614	173.4 ± 403.4
G_5	29	25.4% and 48,080	186.2 ± 440.9
NA	1	11.7% and 22,153	102.4 ± 193.4

beginning of sugar–alcohol plants activities (Fernandes and Correia Filho 2013; IBGE 2018a).

Rainfall over the SoA is generally characterized by strong pluviometric gradients from coast to mainland and from N to S, due to physiography of the region and influence of meteorological systems of different temporal scales. In some regions of Alagoas, in addition to the transition from rainy season to dry season, there is still 1 or 2 months of transition between dry and rainy seasons (Oliveira Júnior et al. 2012; Lyra et al. 2014; Silva 2017). During the driest period in Alagoas (December to February months), the average monthly rainfall is equal to or less than 50 mm, except on the northern part of the state (Lyra et al. 2014). The variability of transition seasons affects the largest fire foci total identified by exploratory analysis in the homogeneous groups.

Rainfall in the state is influenced by multiscale weather systems and by physiography (topography and water bodies), for example, local convection, orographic rains, trade winds (Molion and Bernardo 2002), ITCZ (Gois et al. 2005), UTCV, SL, MCS (Alves et al. 2017), EDW, FS (Moura and Shukla 1981; Lyra et al. 2014, 2017), and maritime–terrestrial breeze circulations (Molion and Bernardo 2002).

Comparatively, the period of greatest fire foci occurrence between the five groups, between September and December months, showed high variability in Alagoas. G_1 (Fig. 5a) has low fire foci occurrence, with values lower than 10 foci month^{-1}, and its maximum between 30 and 62 foci month^{-1}, even though it is one of the largest homogeneous groups. In G_2 (Fig. 5b), the higher fire foci occurrence was recorded with its maximum between 100 and 300 foci month^{-1}.

Such fire foci variability in G_2 is associated with the sugarcane–alcohol industry activities, as well as the urban growth of some municipalities, such as Atalaia, Marechal Deodoro, and Teotônio Vilela (IBGE 2018a, b). G_3 with fire foci occurrence of 100 and 500 foci month^{-1} presents similar behavior to G_4 and G_5. It is important to mention the presence of outliers in all homogeneous groups and NA (Coruripe) in the monthly scale.

In the annual scale, the fire foci homogeneous groups showed different patterns along the time series (Fig. 7), along with several outliers, mainly in G_1 and G_2. For G_1 (Fig. 7a) and G_2 (Fig. 7b), there were no maximum greater than 100 and 200 foci, respectively, and the minimum (maximum) were predominant in both, with a highlight for year 2014 (2016) in both groups. In G_3, the highest fire foci occurrences were registered in 2002, 2004, 2007, and 2010 (Fig. 7c). Contrariwise, G_4 presented the highest fire foci occurrences during the time series, exceptions were years 2000 and 2004 (Fig. 7d).

G_5 (Fig. 7e) presents strong variability in the records of fire foci throughout the series; however, the lowest annual registers were recorded in years 2000, 2001, and 2014. The municipality of *Coruripe* (NA) presents numerous outliers compared with other homogeneous groups and also high fire foci variability in the annual scale (Fig. 7f). The G_2, G_4, and NA (*Coruripe*) groups are associated with the sugarcane harvesting process for the extraction of sugar and ethanol (Fernandes and Correia Filho 2013). While in G_3, besides the sugar and alcohol industry, in some municipalities such as *Pilar*, *Maceió*, *Rio Largo*, and *São Luís do Quitunde*, there was an expressive change in the land use and soil coverage from 2000, caused by urban expansion (Santiago and Gomes 2016).

In addition, all homogeneous groups presented large number of outliers on both scales. Outliers are related to inclusion of new environmental satellites with new orbital sensors for fire foci monitoring. In 1998, there were only two satellites, while currently there are 17 environmental satellites in orbit (Fig. 5c). In addition to the number of environmental satellites, there is also a repetition of fire foci records. All homogeneous groups converge for the year 2014 as the year of the least fire foci occurrence. This pattern is associated with two factors: (i) the decrease in the number of orbital satellites, from 22 satellites in 2013 to 16 satellites in 2014 (CPTEC 2018), and (ii) reduction in harvested area and sugar cane production (Table 4). According

Table 3 Descriptive statistics (minimum, first quartile, median, mean, third quartile, and maximum) of the five homogeneous groups (G_1 to G_5) and the municipality that did not form a group (NA) obtained by the CA technique

Parameters	G_1	G_2	G_3	G_4	G_5	NA
Minimum	0	0	0	0	0	0
1st quartile	0	0	0	0	0	0
Median	12	13	30	18	36	12
Average	79	112	198	173	186	102
3rd quartile	62	112	161	145	148	138
Maximum	1375	1704	3348	3278	3487	1356

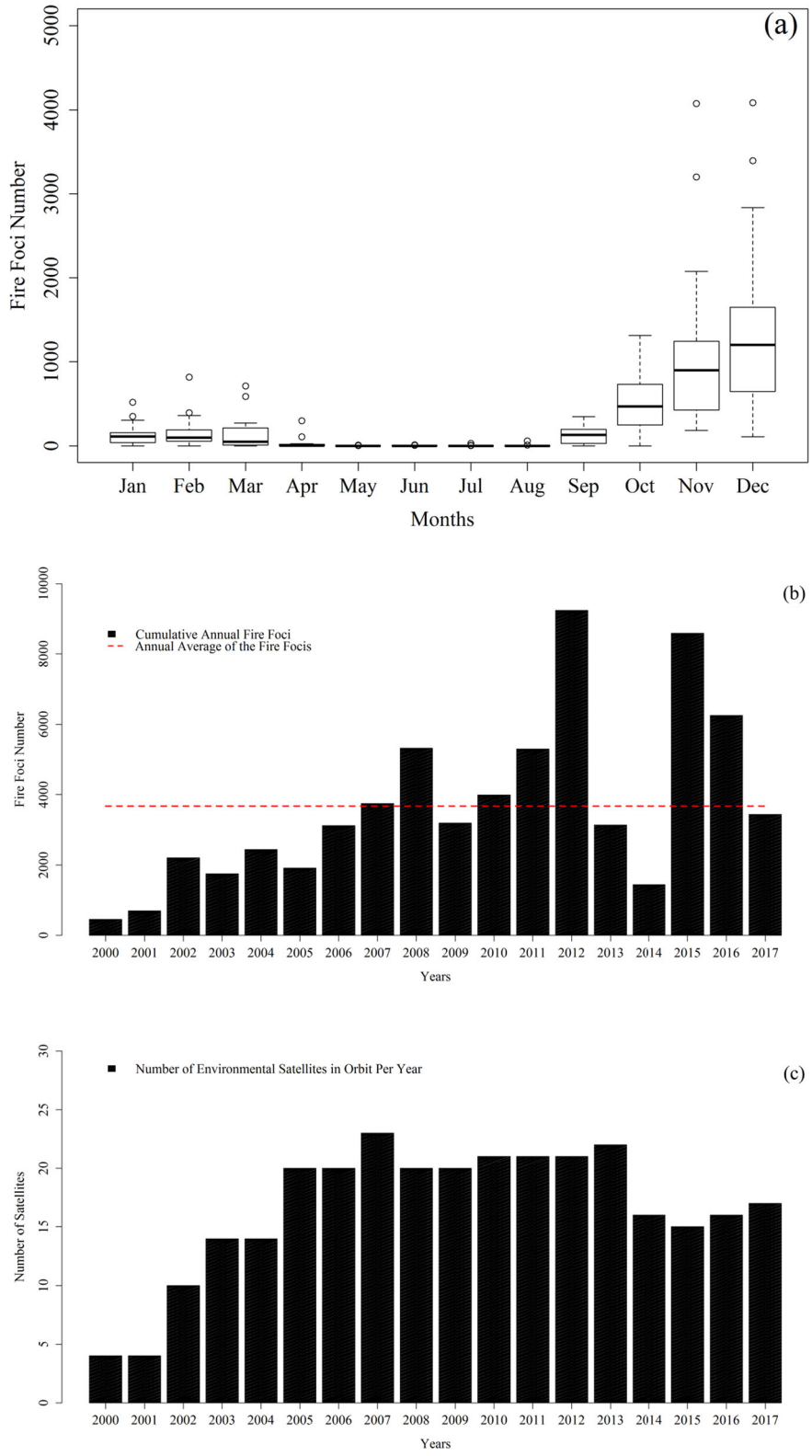

Fig. 5 Boxplot of fire foci on a monthly scale (**a**) for the state of Alagoas. Annual evolution of the number of fire foci (**b**) and satellites in orbit (**c**) for environmental monitoring during the period 2000–2017. The red dotted line corresponds to the average annual fire foci

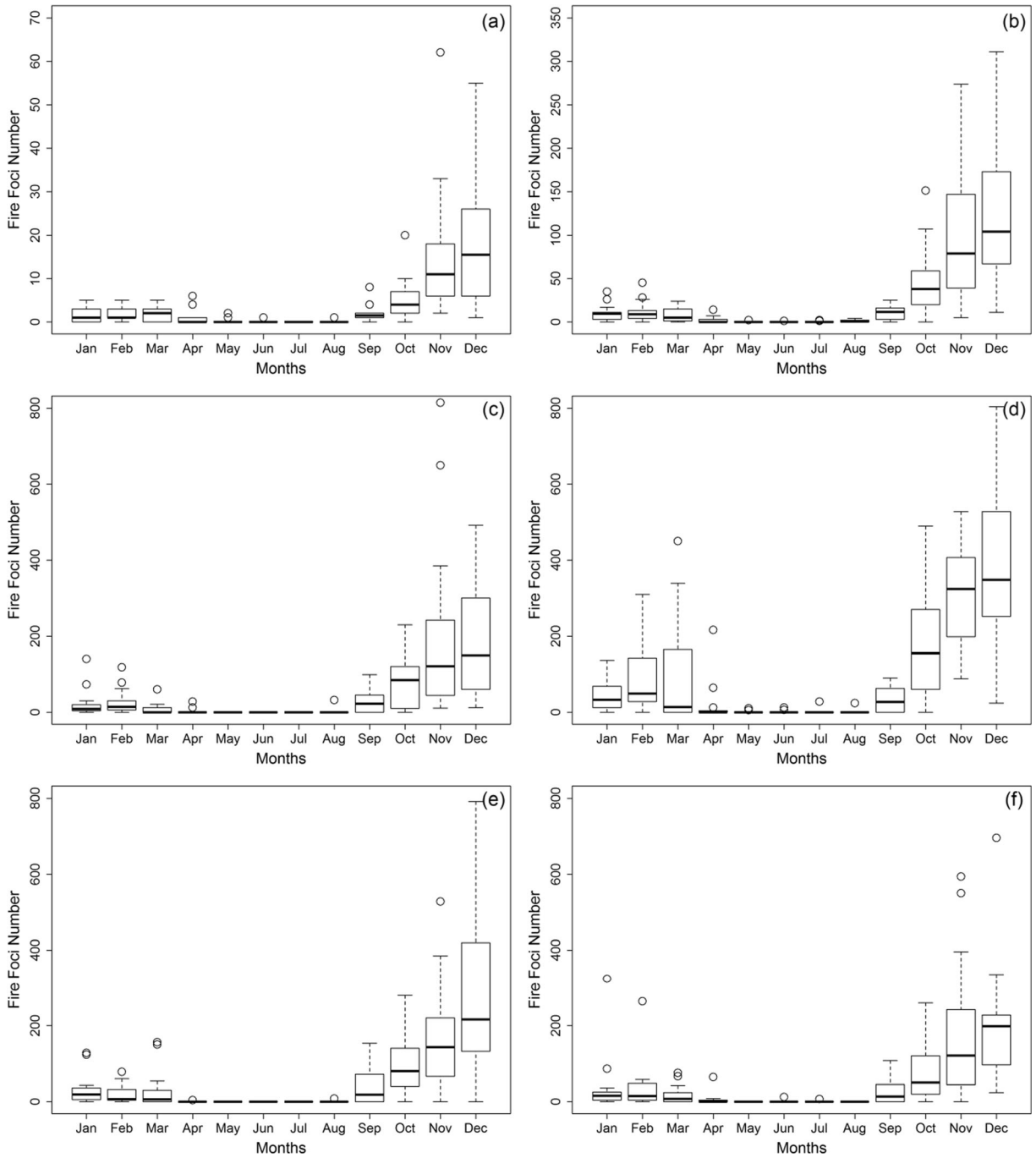

Fig. 6 Boxplot of fire foci corresponding to the five homogeneous groups obtained by the CA: (**a**) G_1, (**b**) G_2, (**c**) G_3, (**d**) G_4, (**e**) G_5, and (**f**) NA

to IBGE's Annual Municipal Agricultural Production data (2018b), G_2 and G_4 presented reduction of harvested area and sugarcane production, which was also registered in *Coruripe* with an intense loss of 7200 ha (13.8%) and 687,000 tons (18.8%) of sugarcane production in 2014.

Two fire foci homogeneous groups (G_2, G_4) and NA, resulting in eight municipalities (*Atalaia*, *Coruripe*,

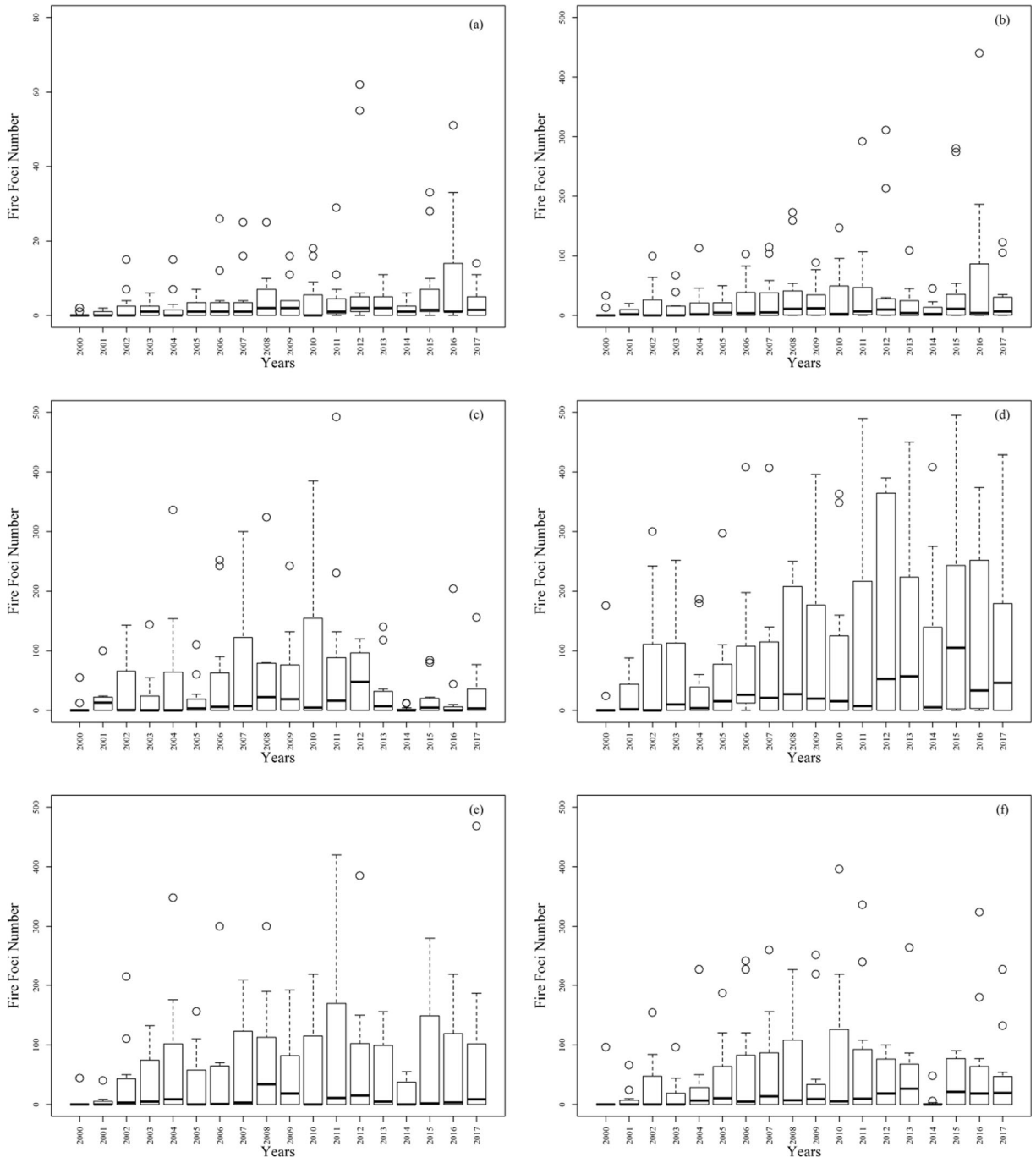

Fig. 7 Annual boxplot of fire foci corresponding to the five homogeneous groups obtained by the CA: (**a**) G_1, (**b**) G_2, (**c**) G_3, (**d**) G_4, (**e**) G_5, and (**f**) NA

Jequiá da Praia, *Penedo*, *Marechal Deodoro*, *São Miguel dos Campos*, and *Teotônio Vilela*) that present high variability along the time series, differently from the G_1 (79 foci month^{-1}) which presented lower variation in both temporal and spatial scales (Figs. 6 and 7). Comparatively, the other groups showed a significant increase, for example, G_2 (137 foci month^{-1}), G_3 (198 foci month^{-1}), G_4 (173 foci month^{-1}), G_5 (186 foci month^{-1}), and NA (102 foci month^{-1}) (Table 3).

Table 4 Harvested area (thousand hectares) and annual production (thousand tons) of sugarcane for each of the homogeneous groups with the highest percentage of fire foci occurrence (G_2, G_4, and NA), from the period 2010 to 2016 for the SoA (IBGE, 2018)

Groups	2010	2011	2012	2013	2014	2015	2016
Harvested area (thousand hectares) of sugarcane							
G_2	63.1	63.1	63.1	65.4	62.0	51.2	50.9
G_3	121.3	121.4	120.9	122.9	113.2	94.4	92.5
G_4	66.5	66.5	66.5	65.7	66.5	40.1	47.1
NA	52.2	52.2	52.2	52.2	45.0	33.5	32.6
Production (thousand tons) of sugarcane							
G_2	3.695	4.393	4.165	4.480	4.089	3.296	2.954
G_3	6.724	8.076	7.645	7.692	7.251	6.706	5.932
G_4	3.734	4.483	4.250	4.258	4.265	2.791	2.830
NA	3.030	3.637	3.448	3.653	2.966	2.184	1.957

Fire foci time series analysis

The fire foci time series of each homogeneous group individually (Fig. 8) present fluctuations, with their maximum starting in 2008. The maximum of G_1 exceeds the average of 2000 foci (Fig. 8a), highlighting the year 2012 (> 6000 foci); unlike the G_2 which registered maxima greater than 1500 fire foci (Fig. 8b), again highlighting the year of 2012 (> 3000 foci yearly). In G_3, with values above the average of 2200 foci, the highlights were the years of 2012, 2015, and 2016 (> 4000 foci per year).

In G_4, the maximum fire foci number exceeded 2200 per year with emphasis on years 2012 and 2015 (> 5000 Foci per year). Finally, in G_5 with maxima higher than the average similar to G_4, highlights were registered also in 2012 (≅ 7000 foci annual) and 2016 (> 5000 foci annual). It is worth observing that up until 2013, new environmental satellites have become available; however, since 2014, the orbital sensors have been modernized for fire foci detection and incorporated into the BDQueimadas (Pereira and Silva 2016; Clemente et al. 2017; CPTEC 2018). Drought severity in SoA (Lyra et al. 2017; Marengo et al. 2017a; Marengo et al. 2017b; Correia Filho et al. 2018) motivated by the ENSO action observed during the years 2008, 2010–2011, 2012, and 2015–2016, which in turn promotes vegetative stress and associated with environmental conditions, triggers the records of fire foci higher than average in all homogeneous groups.

Soil use and coverage

The influence of land use and occupation on the SoA was evaluated for the years 2000 and 2015 based on spatiotemporal results (Table 5). In this approach, the groups with the highest fire foci number and with a smaller number of municipalities were selected. G_2, G_3, G_4, and NA (*Coruripe*), composed of 20 municipalities, represent 64.2% of fire foci occurrence on the SoA. Land use and occupation data presented minimal differences between the 2000 and 2015 (Table 5). It is verified that agricultural crop is the main category of land use and cover with percentages from 45 to 60%, for years 2000 and 2015, respectively. The second most representative category refers to urban areas with values registering an increase from 20 to 39% in the same period. Results shows that the fire foci variability in the SoA is not motivated exclusively by land use and cover changes, since its occurrence percentage has increased more than land use and soil coverage modification.

Poisson regression analysis

Based on the previous results, Poisson regression model was applied to fire foci time series. All the models adopted in the study indicate that covariates have high statistical significance (p value < 0.02). This shows that all the selected variables presented an excellent association with fire foci. In GLM1, the HDI variable stands out due to the direct relation to the fire foci number. In GLM2, composed of variables rainfall and quantity of

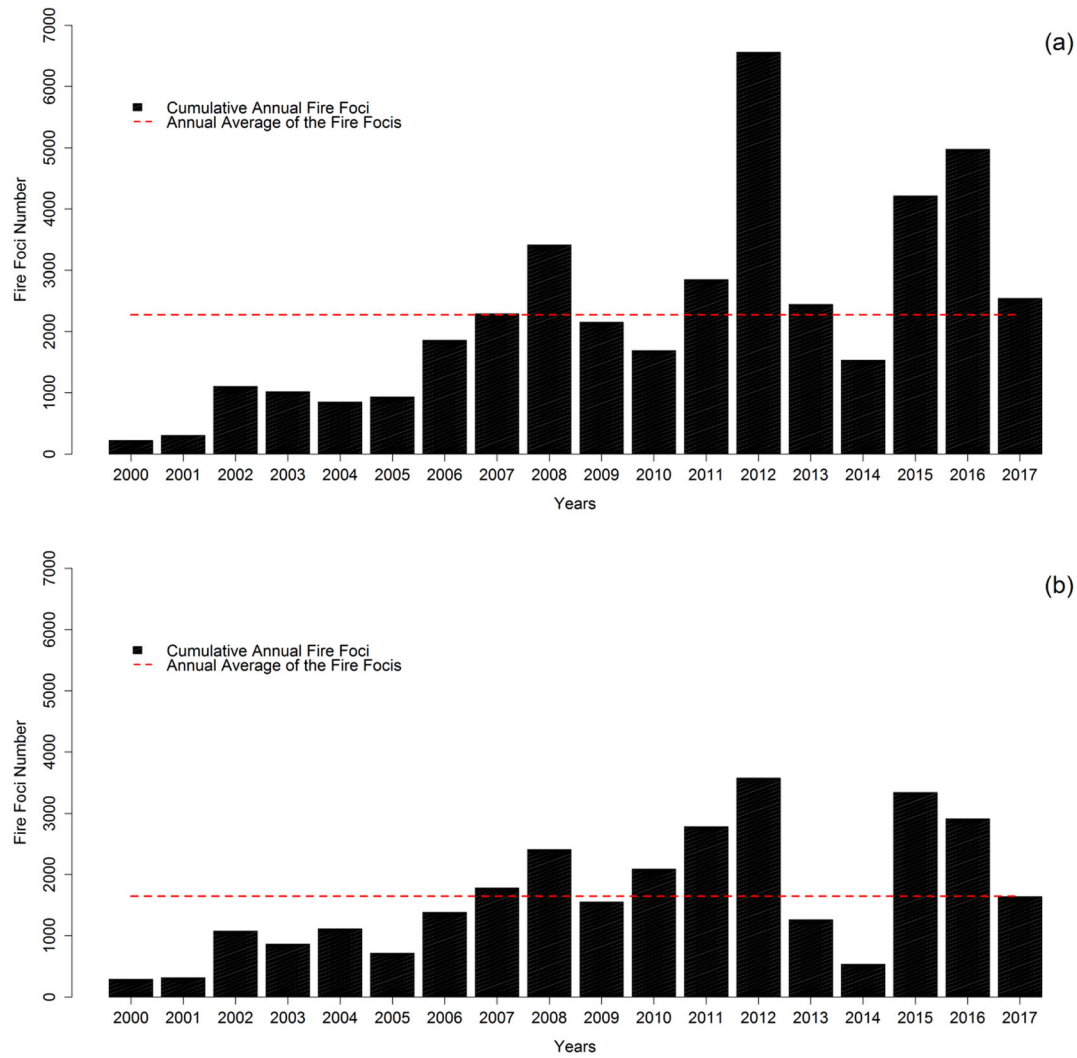

Fig. 8 Boxplot of fire foci corresponding to the five homogeneous groups obtained by the CA: **a** G_1, **b** G_2, **c** G_3, **d** G_4, and **e** G_5. The red dotted line corresponds to the average annual fire foci

sugarcane produced, a significant increase on fire foci occurrence in the state was registered, with direct environmental impacts to the SoA (Table 6).

In GLM3, the combination of socioeconomic and environmental variables showed a greater influence on fire foci occurrence, especially the HDI variable. When analyzing the HDI variable alone (model GLM4), it was verified that the result shows similar behavior to GLM1 and GLM3. The residual analysis (residual deviance and AIC) and the percentage of the extracted variance (R^2) showed that GLM4 has 57.3% of the variance explained. This shows the importance of HDI, previously verified for GLM1 and GLM3. Although the variance value of GLM4 is strongly affected by noise, according to the AIC value (2572.0) and residual deviance (2453.5), this is due to the low number of data (16 elements) used in the regression model.

The contrast between GLM1 and GLM2 showed that socioeconomic variables (residual deviance = 39.1, AIC = 110.8, and $R^2 = 85.4\%$) had greater influence, followed by precision in their prediction than the environmental variables (residual deviance = 1697.8, AIC = 1824.3, and $R^2 = 66.8\%$), respectively. GLM3 presented the lowest values (residual deviance = 845.3 and AIC = 975.7) and $R^2 = 80.3\%$. The GLM results show that the regional development and economic growth (HDI) are main responsible variables for the increase of fire foci occurrence in the SoA. This process of regional

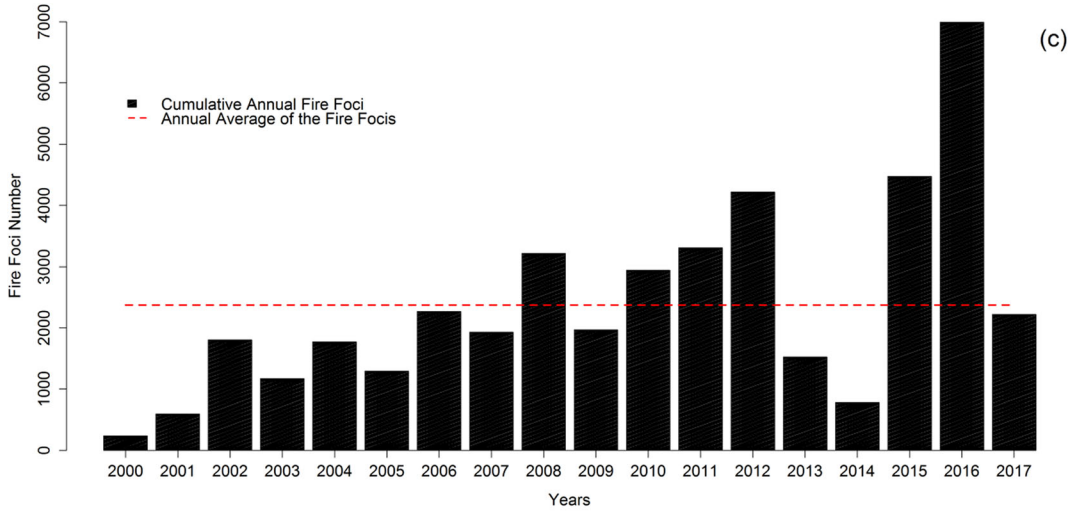

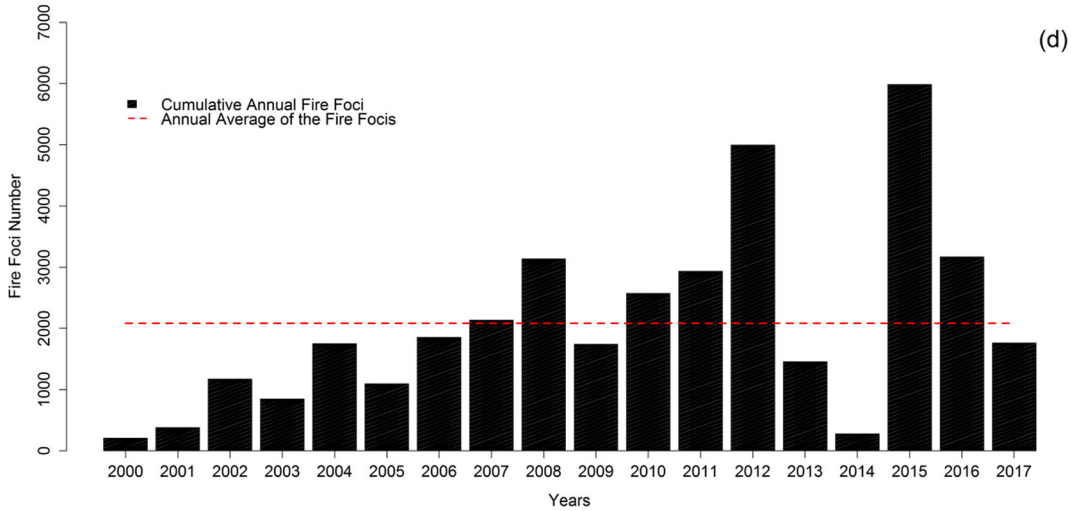

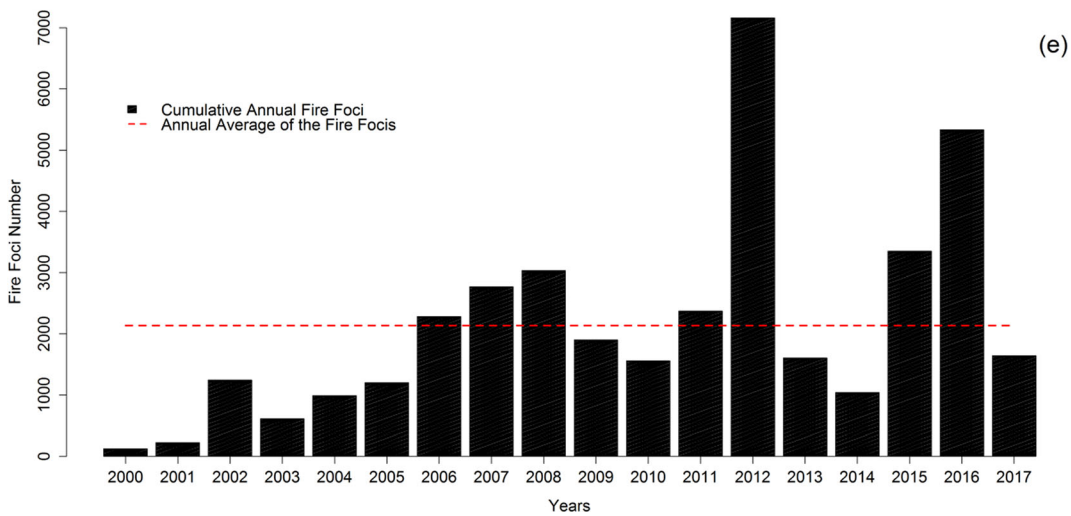

Fig. 8 (continued)

development and redistribution of the population contingent led to problems in land use and occupation as verified by Correia Filho et al. (2019b) and Hammer et al. (2009), in addition to degradation in environmental protection areas as reported by Silva Lopes et al. (2018) in the municipality of Maceió, the capital of SoA.

Principal component analysis

Based on the results of the PCA, the KMO test assured good quality (0.72) to the data matrix and therefore suitable for the study. In addition, the chi-square and *p* value tests presented significant statistical values, being 1318.93 and < 0.001, respectively. Through the Kaiser method ($\lambda > 1$), three principal components were extracted which in total 78.70% of the explained variance (Table 7). Regarding the variability of the variables via biplot (Fig. 9), it showed positive correlations between variables GDP, population, and demographic density, for PC1 and PC2, with contributions greater than 13.74% for each. With positive correlations to PC1 and negative correlations to PC2, there are also other variables, such as fire foci, crop production, and cropland area with contributions ranging from 8.10 to 14.90%. This configuration showed that the increase of fire foci is strongly related to the growth of the cultivated area and sugarcane production in the SoA and is corroborated by the results obtained by Fernandes and Correia Filho (2013).

In a joint analysis between the municipalities and the variables, it appears that the municipalities behave alike regarding the occurrence of fire foci—cropland area, crop production, and income—which in turn are directly associated with the clusters of higher records of fire foci in the SoA (Fig. 10). For example, the capital of the state, the municipality of Maceió (corresponding to point 47, located in the upper right) presented high association of fire foci with GDP, population, and demographic density.

Regarding the percentage load of each PC (Table 7), it is observed that PC1 explains 42.30%, and the largest contributions are associated with the demographic variables, in this case, population, GDP, and demographic density with values of 13.74%, 13.74%, and 13.19%, respectively. In both PCs, the number of fire foci does not emerge as a major variable. In the case of PC3, Gini index, rainfall, and fire foci appear as the main variables, with values of 51.84%, 27.32%, and 10.36%, respectively.

The results obtained with the PCA technique showed marked differences and also similar results via GLM, highlighting the synthesis of data via PCA compared with GLM. In the case of PCA, each variable was individually assessed, but revealed a good association between fire foci, sugarcane production, and harvested area, followed by a similar relationship between PC3 and cluster 3. The authors also point out that such changes affect ecosystems, as well as changes in land use and natural resources. In this respect, Brazil, including SoA, a large part of the population is concentrated on the coast, where it used to be the Atlantic Forest biome, deforested to meet the process of expansion and development (Oliveira Souza et al. 2018).

Table 5 Average percentage of soil cover for the homogeneous groups with the highest percentage of fire foci occurrence (G_2, G_3, G_4, and NA) between years 2000 and 2015

Soil cover type	(%)			
	G_2	G_3	G_4	NA
Rainfed cropland	54	45	60	49
Herbaceous Cover	1	0	1	1
Cropland (> 50%)/natural vegetation (< 50%)	12	6	4	4
Natural vegetation (> 50%)/cropland (< 50%)	5	4	5	7
Tree cover, broadleaved, evergreen, open (> 15%)	1	2	4	4
Tree and shrub (> 50%)/herbaceous cover (< 50%)	0	1	0	0
Herbaceous cover (> 50%)/tree and shrub (< 50%)	0	0	1	1
Shrubland	1	0	0	0
Grassland	1	2	2	1
Urban areas	25	39	20	31
Water resources	0	1	0	0

Conclusions

The CA applied to fire foci time series based on the Ward method identified five homogeneous groups in the SoA (G_1 to G_5) and a municipality (*Coruripe*) that did not adhere to any group. The result obtained by CA presented consistency according to the cophenetic correlation coefficient (> 0.70). G_1 and G_5 registered the largest number of municipalities with fire foci in the state, with 53 and 29, respectively. G_2, G_3, and G_4

Table 6 Poisson regression models created from the homogeneous groups with the highest percentage of fire foci occurrence (G_2, G_4, and NA), where model 1 consists of socioeconomic variables, model 2 consists of environmental variables, model 3 is the junction of models 1 and 2, and model 4 only by the HDI

Variables	Model 1 Coeff ± SE	Model 2 Coeff ± SE	Model 3 Coeff ± SE	Model 4 Coeff ± SE
Intercept	1.0 ± 0.2***	7.3 ± 0.0***	3.3 ± 0.1***	1.1 ± 0.1***
Population size	0.0 ± 0.0***	–	− 0.0 ± 0.0***	–
Total area	− 0.0 ± 0.0***		− 0.0 ± 0.0***	
Demographic density	− 0.0 ± 0.0***	–	− 0.0 ± 0.0***	–
HDI	13.6 ± 0.3***	–	10.4 ± 0.3***	–
Gini index	–	–	–	9.1 ± 0.2***
Per capita	− 0.0 ± 0.0***	–	0.0 ± 0.0*	–
Rainfall	–	− 0.0 ± 0.0***	0.0 ± 0.0***	–
Cropland area	–	0.0 ± 0.0***	–	–
Crop production	–	− 0.0 ± 0.0***	− 0.0 ± 0.0***	–
Variance and residual analysis				
Residual deviance	1697.8	4215.6	845.3	2453.5
AIC	1824.3	4338.1	975.7	2572.0
R^2 (%)	66.4	25.2	80.3	57.3

Coeff regression coefficient, *SE* standard error, *AIC* Akaike information criterion, R^2 determination coefficient

Model GLM1: population size + demographic density + total area + HDI + per capita. Model GLM2: rainfall + produced quantity (sugarcane). Model GLM3: population size + demographic density + total area + HDI + rainfall + per capita + produced quantity (sugarcane). Model GLM4: Gini index

The asterisks represent the statistical significance levels: (***) from 0 and 0.001, (**) from 0.001 and 0.01, (*) from 0.01 and 0.05, and (.) from 0.05 to 0.1

together account only for 20 municipalities, although they detected about 52.5% of total foci occurrences (99,200). G_3 (with only three municipalities) and *Coruripe* have 60,767 fire foci (32.1%), with a total of 38,614 foci (20.4%) and 22,153 foci (11.7%), respectively. The spatial distribution and concentration of homogeneous groups of minor fire foci are associated with the *Litoral*, BSF, and ZM regions. The largest groups are distributed throughout the state of Alagoas, especially in the *Litoral* region. In this region, the highest records of fire foci are located in municipalities with sugarcane planting areas and sugar–alcohol mills installed.

Table 7 Evaluation of the percentage in the contribution of the analyzed variables in each of the four main components and their respective explained variance and total variance (both in %)

Variables	PC1	PC2	PC3
Fire foci	8.12	13.37	10.36
Rainfall	7.52	1.65	27.32
Gini	0.01	7.32	51.84
Population	13.74	14.97	0.08
GDP	13.74	14.55	0.00
Income	8.68	2.29	2.27
HDI	11.10	0.56	0.21
Demographic density	13.19	15.63	0.51
Cropland area	12.07	14.92	3.67
Crop production	11.83	14.74	3.75
Variance explained (%)	42.30	25.30	11.20
Total variance explained (%)	42.30	67.60	78.80

On the monthly scale, all groups recorded the highest totals of fire foci in the last quarter of the year—September to December months—except G_4 which registered highest fire foci totals from January to March. This seasonal pattern presented by the G4 is similar to that of the neighboring state, Sergipe, with significant variations. The 4-month period identified in the study corresponds to the transition from rainy season to the dry season. During this period, the average monthly rainfall is equal or less

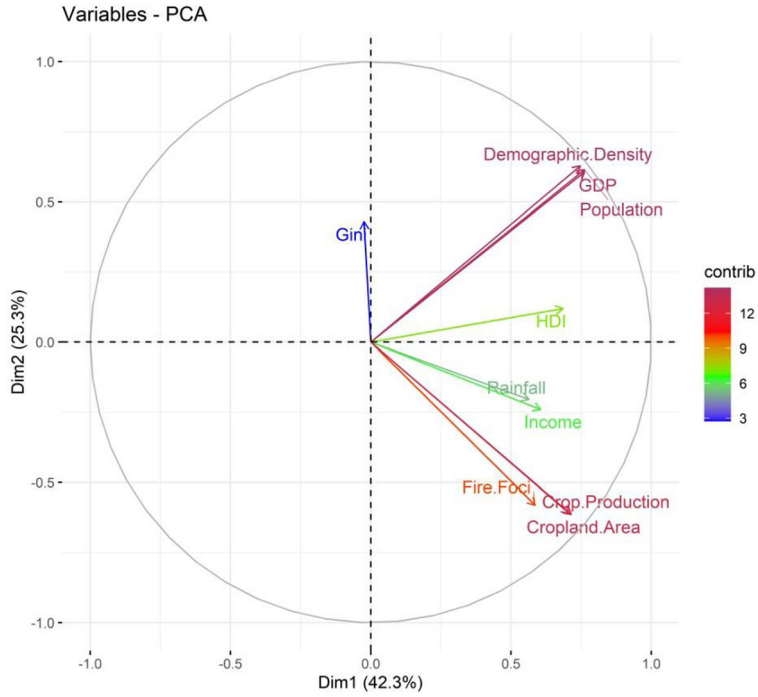

Fig. 9 Correlation coefficient chart for the first two PCs. The color of the arrows corresponds to the degree of contribution of the variable given in (%): the color blue for the lowest and red for the highest

than 50 mm and associated with the beginning of the sugar–alcohol industry activities in the state, interfering greatly in the fire foci dynamics.

In annual scale, all groups registered high number of outliers, due to inclusion of new environmental satellites with new orbital sensors for fire foci monitoring. The inclusion of new environmental satellites from the beginning of the series up to 2013 must be noticed. Outliers also varied according to production levels of the sugar–alcohol industry in the SoA. The intense drought that started between years 2010 and 2011 favored fire foci occurrence in subsequent years (2011, 2012, 2015,

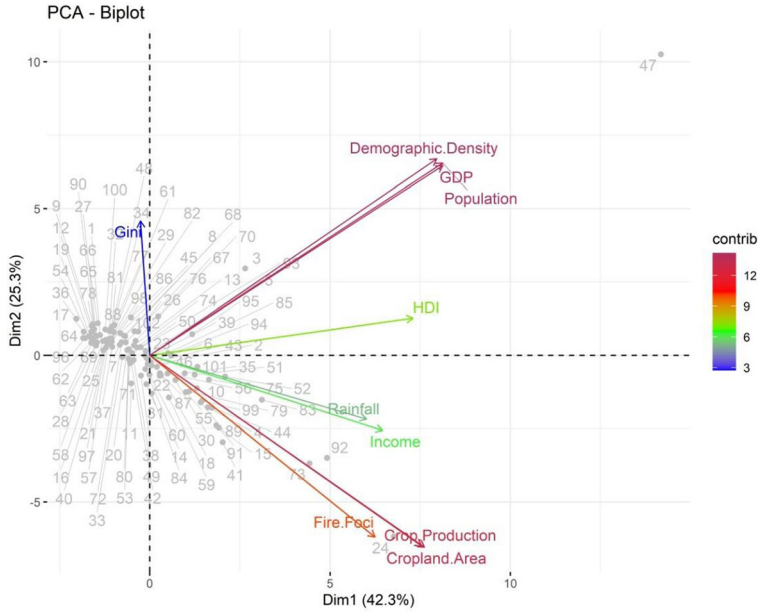

Fig. 10 Biplot of scores for the first two PCs for the ten variables and 102 municipalities used in this study

and 2016) in all homogeneous groups. This drought is due to the phases of ENSO, La Niña (2011/2012), and El Niño (2015/2016) and prolonged between 2012 and 2015 in NEB, including Alagoas, which are determinant in the significant increase of fire foci.

The Fire Foci variability in the largest homogeneous groups is restricted to only two categories of land use and cover, agricultural crops (mainly sugarcane), followed by urban areas category. Such variability is not motivated by changes in soil use and cover. The result of the generalized linear model via Poisson regression shows that the variability of fire foci is strongly associated with socioeconomic variables such as HDI and Gini index.

The PCA technique reinforces the use of multivariate statistics in relational pattern analysis between fire foci and socioeconomic and environmental variables in SoA, especially individually. The PCA captured three PCs, with 78.80% of the variance explained. PC1 holds 42.30%, and is influenced by population, GDP, and demographic density. On the municipal scale, Maceió holds 46.60% and 40.85% for PC1 and PC2. Urban densification and population growth contribute to profound changes not only in the record of fire foci but also in land use and occupation and natural resources, especially in what remains of the Atlantic Forest biome.

Fire foci orbital monitoring via environmental satellites is an important tool in identifying critical areas during the transition from the rainy season to the dry season and at the beginning of sugar–alcohol industry activities in the state. Its use in a routine manner by public managers could contribute to fire prevention and control policies, especially in municipalities with higher concentration rates of fire foci in the state of Alagoas.

As a future proposal, it is interesting to evaluate the effects of burning by burning sugarcane straw on atmospheric pollution and worsening air quality in the state of Alagoas based on remote sensing and numerical modeling products.

Acknowledgments The authors are grateful to the Center for Weather Forecasting and Climate Studies/National Institute of Space Research (CPTEC/INPE) for making available the fire foci data via BDQueimadas data bank. The authors also thank ESA of the CCI-CL group for making available the world's coverage data via annual maps version 2.0.7. The first author thanks the research productivity scholarship granted by the National Council of Scientific and Technological Development (CNPq) process number 309681/2019-7. The authors also thank CNPq for the funding project 424605/2018-0—linked to the Universal Notice No. 28/2018. The second author thanks CNPq for the Junior Postdoctoral Scholarship No. 161023/2019-3.

References

Akaike, H. (1974). A new look at the statistical model identification. *IEEE Transactions on Automatic Control, 19,* 716–723.

Alencar, A. A., Solórzano, L. A., & Nepstad, D. C. (2004). Modeling forest understory fires in an eastern Amazonian landscape. *Ecological Applications, 14*, 139–149. https://doi.org/10.1890/01-6029.

Alves, J. M. B., Silva, E. M., Sombra, S. S., Barbosa, A. C. B., & Santos, A. C. S. (2017). Eventos Extremos Diários de Chuva no Nordeste do Brasil e Características Atmosféricas. *Revista Brasileira de Meteorologia, 32*, 227–233. https://doi.org/10.1590/0102-77863220012.

Barros Santiago, D., Correia Filho, W. L. F., Oliveira-Júnior, J. F., & Junior, S. (2019). Mathematical modeling and use of orbital products in the environmental degradation of the Araripe Forest in the Brazilian northeast. *Modeling Earth Systems and Environment, 5*, 1429–1441. https://doi.org/10.1007/s40808-019-00614-x.

Barros, A.H.C., Araújo Filho, J.C., Silva, A.B., & Santiago, G.A.C.F. (2012). Climatologia do Estado de Alagoas. Dados eletrônicos. Recife: Embrapa Solos.

Belo, C., & Santos, S. S. (2013). A paisagem canavieira em União dos Palmares-Alagoas e seus impactos socioambientais. *Revista Ambientale, 4*, 1–13.

Bem, P. P., Carvalho Júnior, O. A., Trondoli, M. E. A., Guimarães, R. F., & Gomes, R. A. T. (2018). Predicting wildfire vulnerability using logistic regression and artificial neural networks: a case study in Brazil's Federal District. *International Journal of Wildland Fire, 28*, 35–45. https://doi.org/10.1071/WF18018.

Biagiotti, D., Sarmento, J. L. R., Rego Neto, A. A., Santos, G. V., Silva Santos, N. P., Torres, T. S., & Neri, V. S. (2013). Caracterização fenotípica de ovinos da raça Santa Inês no Estado do Piauí. *Revista Brasileira de Saúde e Produção Animal, 14*, 29–42. https://doi.org/10.1590/S1519-99402013000100004.

Bontemps, S., et al. (2015). Multi-year global land cover mapping at 300 M and characterization for climate modelling: achievements of the land cover component of the ESA climate change initiative. ISPRS Arch. 40-7W3, 323–328. https://doi.org/10.5194/isprsarchives-XL-7-W3-323-2015.

Brando, P. M., Balch, J. K., Nepstad, D. C., Morton, D. C., Putz, F. E., Coe, M. T., Silvério, D., Macedo, M. N., Davidson, E. A., Nóbrega, C. C., Alencar, A., & Soares-Filho, B. S. (2014). Abrupt increases in Amazonian tree mortality due to drought-fire interactions. *Proceedings of the National Academy of Sciences, 111*, 6347–6352. https://doi.org/10.1073/pnas.1305499111.

Caúla, R. H., Oliveira-Júnior, J. F., Lyra, G. B., Delgado, R. C., & Heilbron Filho, P. F. L. (2015). Overview of fire foci causes and locations in Brazil based on meteorological satellite data from 1998 to 2011. *Environmental Earth Sciences, 74*, 1497–1508. https://doi.org/10.1007%2Fs00703-016-0481-x.

Caúla, R. H., Oliveira-Júnior, J. F., Gois, G., Delgado, R. C., Pimentel, L. C. G., & Teodoro, P. E. (2016). Nonparametric statistics applied to fire foci obtained by meteorological satellites and their relationship to the MCD12Q1 product in the state of Rio de Janeiro, Southeast

- Brazil. *Land Degradation & Development, 28*, 1056–1067. https://doi.org/10.1002/ldr.2574.

Chuvieco E., Aguado I., Jurdao S., Pettinari M. L., Yebra M., Salas J., et al. (2012). Integrating geospatial information into fire risk assessment. *International Journal of Wildland Fire, 23,* 606–619. https://doi.org/10.1071/WF12052.

Clemente, C. (2011). Aspectos da vida comunitária e da cultura política de um assentamento rural em Murici: reflexões em torno de uma das comunidades visitadas pela equipe da UFU no Projeto Rondon em Alagoas. *Revista Em Extensão, 9*, 2.

Clemente, S. S., Oliveira Júnior, J. F., & Louzada, M. A. P. (2017). Focos de Calor na Mata Atlântica do Estado do Rio de Janeiro. *Revista Brasileira de Meteorologia, 32*, 669–677. https://doi.org/10.1590/0102-7786324014.

Corrar, L.J., Paulo, E., & Dias Filho, J.M. (2007). Análise Multivariada - Para os Cursos de Administração, Ciências Contábeis e Economia, Ed. Atlas, São Paulo, 1ª Edição, 344 p.

Correia Filho, W. L. F., & Silva Aragão, M. R. (2014). Padrões Temporais do Vento à Superfície em Mesorregiões do Estado da Bahia. *Ciência e Natura, 36*, 402–414.

Correia Filho, W. L. F., Lucio, P. S., & Spyrides, M. H. C. (2016). Caracterização dos Extremos de Precipitação diária no Nordeste do Brasil. *Boletim Goiano de Geografia, 36*(3), 539–554. https://doi.org/10.5216/bgg.v36i3.44557.

Correia Filho, W. L. F., Santos, T. V., Diogo, A. M., & Amorim, R. F. C. (2018). Diagnóstico da Precipitação e EVI em Dois Eventos de Seca no Nordeste do Brasil. *Revista do Departamento de Geografia, 35*, 102–112. https://doi.org/10.11606/rdg.v35i0.140068.

Correia Filho, W. L. F., Oliveira-Júnior, J. F., Barros Santiago, D., Terassi, P. M. B., Teodoro, P. E., Gois, G., Blanco, C. J. C., Souza, P. H. A., Costa, M., & Santos, P. J. (2019a). Rainfall variability in the Brazilian northeast biomes and their interactions with meteorological systems and ENSO via CHELSA product. *Big Earth Data, 3*, 315–337. https://doi.org/10.1080/20964471.2019.1692298.

Correia Filho, W. L. F., Barros Santiago, D., Oliveira-Júnior, J. F., & Silva Junior, C. A. (2019b). Impact of urban decadal advance on land use and land cover and surface temperature in the city of Maceió, Brazil. *Land Use Policy, 87*, 104026. https://doi.org/10.1016/j.landusepol.2019.104026.

CPTEC—Centro de Previsão do Tempo e Estudos Climáticos. (2018). BDQUEIMADAS. http://pirandira.cptec.inpe.br/queimadas/. Accessed 14 Feb 2018.

ESA – European Space Agency. (2018). Climate Change Initiative, Land Cover Maps - v2.0.7, Land Covers Maps 2000 and 2015. https://storage.googleapis.com/cci-lc-v207/ESACCI-LC-L4-LCCS-Map-300m-P1Y-1992_2015-v2.0.7.zip. Accessed 14 Apr 2018.

Eugenio, F. C., Santos, A. R., Pedra, B. D., Pezzopane, J. E. M., Mafia, R. G., Loureiro, E. B., Martins, L. D., & Saito, N. S. (2019). Causal, temporal and spatial statistics of wildfires in areas of planted forests in Brazil. *Agricultural and Forest Meteorology, 266*, 157–172. https://doi.org/10.1016/j.agrformet.2018.12.014.

Everitt, B. S., & Dunn, G. (1991). *Applied multivariate analysis* (400p). London: Edward Arnold.

Fernandes, R. C., & Correia Filho, W. L. F. (2013). Espacialização temporal dos focos de queimadas e de poluentes atmosféricos (CO, CH_4, NO_2, N2O) em Alagoas. *Ciência e Natura, 35*, 287–294. https://doi.org/10.5902/2179460X12580.

Flanningan, M. D., Stocks, B. J., & Wotton, B. M. (2000). Climate change and forest fires. *Science of the Total Environment, 262*, 221–229. https://doi.org/10.1016/S0048-9697(00)00524-6.

Forino, G., von Meding, J., & Brewer, G. J. (2015). A conceptual governance framework for climate change adaptation and disaster risk reduction integration. *International Journal of Disaster Risk Science, 6*, 372–384. https://doi.org/10.1007/s13753-015-0076-z.

Funk, C., Pete, P., Martin, L., Diego, P., James, V., Shraddhanand, S., Gregory, H., James, R., Laura, H., Andrew, H., & Joel, M. (2015). The climate hazards infrared precipitation with stations—a new environmental record for monitoring extremes, California-USA. *Scientific Data, 2*, 10–66. https://doi.org/10.1038/sdata.2015.66.

Gois, G., Souza, J. L., Silva, P. R. T., & Oliveira-Júnior, J. F. (2005). Caracterizacão da desertificação no estado de Alagoas utilizando variáveis climáticas. *Revista Brasileira de Meteorologia, 20*, 301–314.

Hammer, R. B., Stewart, S. I., & Radeloff, V. C. (2009). Demographic trends, the wildland–urban interface, and wildfire management. *Society & Natural Resources An International Journal, 22*, 777–782. https://doi.org/10.1080/08941920802714042.

Harzallah, A., Rocha de Aragão, J. O., & Sadourny, R. (1996). Interannual rainfall variability in North–East Brazil: observation and model simulation. *International Journal of Climatology, 16*, 861–878. https://doi.org/10.1002/(SICI)1097-0088(199608)16:8<861::AID-JOC59>3.0.CO;2-D.

Heinl, M., Silva, J., Tacheba, B., & Bredenkamp, G. J. (2004). Vegetation changes after single fire-events in the Okavango Delta wetland, Botswana. *South African Journal of Botany, 70*(5), 695–704.

Hongyu, K., Sandanielo, V. L. M., & Oliveira Junior, G. J. (2016). Análise de componentes principais: resumo teórico, aplicação e interpretação. *E&S Engineering and Science, 5*, 83–90. https://doi.org/10.18607/ES201653398.

IBGE - Instituto Brasileiro de Geografia e Estatística. (2018a). Censos 2000 e 2010, https://ww2.ibge.gov.br/home/estatistica/populacao/censo2010/indicadores_sociais_municipais/. Accessed 13 Apr 2018.

IBGE - Instituto Brasileiro de Geografia e Estatística. (2018b). Censo Agropecuário, https://www.ibge.gov.br/estatisticas-novoportal/economicas/agricultura-e-pecuaria/9117-producao-agricola-municipal-culturas-temporarias-e-permanentes.html?=&t=downloads. Accessed 13 Apr 2018.

Jiang, Z., Lian, Y., & Qin, X. (2014). Rocky desertification in Southwest China: impacts, causes, and restoration. *Earth-Science Reviews, 132*, 1–12. https://doi.org/10.1016/j.earscirev.2014.01.005.

Justino, F., Peltier, W. R., & Barbosa, H. A. (2010). Atmospheric susceptibility to wildfire occurrence during the Last Glacial Maximum and mid-Holocene. *Palaeogeography, Palaeoclimatology, Palaeoecology, 295*, 76–88. https://doi.org/10.1016/j.palaeo.2010.05.017.

Kayano, M. T., & Andreoli, R. V. (2006). Relationships between rainfall anomalies over northeastern Brazil and the El Nin o

Southern Oscillation. *Journal of Geophysical Research, 111,* D13101. https://doi.org/10.1029/2005JD006142.

Kayano, M. T., & Capistrano, V. B. (2014) . How the Atlantic multidecadal oscillation (AMO) modifies the ENSO influence on the South American rainfall. *International Journal of Climatology, 34,* 162–178. https://doi.org/10.1002/joc.3674.

Kayano, M. T., Andreoli, R. V., & Souza, R. A. F. (2013). Relations between ENSO and the South Atlantic SST modes and their effects on the South American rainfall. *International Journal of Climatology, 33,* 2008–2023. https://doi.org/10.1002/joc.3569.

Kouadio, Y. K., Servain, J., Machado, L. A. T., & Lentini, A. D. (2012). Heavy rainfall episodes in the Eastern Northeast Brazil linked to large-scale ocean-atmosphere conditions in the tropical Atlantic. *Advances in Meteorology, 1-16*.

Lall, S., & Mathibela, B. (2016). The application of artificial neural networks for wildfire risk prediction. In: 2016 International Conference on Robotics and Automation for Humanitarian Applications (RAHA) (pp. 1-6). IEEE. https://doi.org/10.1109/RAHA.2016.7931880.

Lima, M., Vale, J. C. E., Medeiros Costa, G., Santos, R. C., Correia Filho, W. L. F., Gois, G., Oliveira Junior, J. F., Teodoro, P. E., Rossi, F. S., & Silva Junior, C. A. (2020). The forests in the indigenous lands in Brazil in peril. *Land Use Policy, 90*, 104258. https://doi.org/10.1016/j.landusepol.2019.104258.

Lyra, G. B., Santos, M. J., Souza, J. L., Lyra, G. B., & Santos, M. A. (2011). Espacialização da temperatura do ar anual no estado de Alagoas com diferentes modelos digitais de elevação e resoluções espaciais. *Ciência Florestal, 21*, 275–287. https://doi.org/10.5902/198050983231.

Lyra, G. B., Oliveira-Júnior, J. F., & Zeri, M. (2014). Cluster analysis applied to the spatial and temporal variability of monthly rainfall in Alagoas State, northeast of Brazil. *International Journal of Climatology, 34*, 3546–3558. https://doi.org/10.1002/joc.3926.

Lyra, G. B., Oliveira-Júnior, J. F., Gois, G., Cunha-Zeri, G., & Zeri, M. (2017). Rainfall variability over Alagoas under the influences of SST anomalies. *Meteorology and Atmospheric Physics, 129*, 157–171. https://doi.org/10.1007%2Fs00703-016-0461-1.

Malik, K. (2013). Human development report 2013—the rise of the south: human progress in a diverse world. Online at http://hdr.undp.org/en/2013-report, p 216.

Marengo, J. A., Torres, R. R., & Alves, L. M. (2017a). Drought in Northeast Brazil—past, present and future. *Theoretical and Applied Climatology, 129*, 1189–1200. https://doi.org/10.1007/s00704-016-1840-8.

Marengo, J. A., Alves, L. M., Alvala, R. C. S., Cunha, A. P., Brito, S., & Moraes, O. L. L. (2017b). Climatic characteristics of the 2010-2016 drought in the semiarid Northeast Brazil region. *Anais da Academia Brasileira de Ciências, 90*, 1973–1985. https://doi.org/10.1590/0001-3765201720170206.

Melo, M.G.D.S. (2011). Gestão ambiental no setor sucroalcooleiro de Pernambuco: entre a inesgotabilidade dos recursos naturais e os mecanismos de regulação (Master's thesis, Universidade Federal de Pernambuco).

Molion, L. C. B., & Bernardo, S. O. (2002). Uma revisão da dinâmica das chuvas no Nordeste Brasileiro. *Revista Brasileira de Meteorologia, 17*, 1–10.

Mollmann Júnior, R. A., Silva Junior, R. S., Coelho, S. M. S. C., & Medina, B. L. (2015). Estudo da dispersão de monóxido de carbono emitido por queimadas na Amazônia Legal em 19 agosto de 2010 baseado em: Simulações do modelo WRF-Chem e sensoriamento remoto. *Ciência e Natura, 37*, 144–152. https://doi.org/10.5902/2179460X16230.

Moreno, M. V., & Chuvieco, E. (2013). Characterising fire regimes in Spain from fire statistics. *International Journal of Wildland Fire, 22*(3), 296–305.

Moura, A. D., & Shukla, J. (1981). On the dynamics of droughts in Northeast Brazil—observations, theory and numerical experiments with a general-circulation model. *Journal Atmospheric Science, 38*, 2653–2675. https://doi.org/10.1175/1520-0469(1981)038\2653:Otdodi[2.0.Co;2.

Nelder, A. J. A., & Wedderburn, R. W. M. (1972). Generalized linear models. *Journal of the Royal Statistical Society Series A (General), 135*(3), 370–384.

Neves, J.A., Santos, C.C., Amaral, A.F.C., Sant'anna, S.A.C., Silva, P.A., & Ivo Mello, W.P. (2018). Emissões de gases de efeito estufa em áreas de cana-de-açúcar colhida crua e queimada. In: Embrapa Tabuleiros Costeiros-Artigo em anais de congresso (ALICE). In: Seminário De Iniciação Científica E Pós-Graduação Da Embrapa Tabuleiros Costeiros, 8., 2018, Aracaju. Anais... Aracaju: Embrapa Tabuleiros Costeiros, 2018. Editor técnico: Ronaldo Souza Resende., 2018.

Oliveira Júnior, J. F., Lyra, G. B., Gois, G., Brito, T. T., & Moura, N. S. H. (2012). Análise de homogeneidade de séries pluviométricas para determinação do índice de seca IPP no estado de Alagoas. *Floresta e Ambiente, 19*, 101–112. https://doi.org/10.4322/floram.2012.011.

Oliveira Souza, T. C., Delgado, R. C., Magistrali, I. C., Santos, G. L., Carvalho, D. C., Teodoro, P. E., Silva Junior, C. A., & Caúla, R. H. (2018). Spectral trend of vegetation with rainfall in events of El Niño-Southern Oscillation for Atlantic Forest biome, Brazil. *Environmental Monitoring and Assessment, 190*, 688–698. https://doi.org/10.1007/s10661-018-7060-1.

Oliveira-Júnior, J. F., Sousa, G. M., Nunes, M. T. O., Fernandes, M. C., & Tomzhinski, G. W. (2017). Relationship between SPI and ROI in Itatiaia National Park. *Floresta e Ambiente, 24*, e20160031. https://doi.org/10.1590/2179-8087.003116.

Oliveira-Júnior, J. F., Teodoro, P. E., Silva Junior, C. A., Rojo Baio, F. H., Gava, R., Capristo-Silva, G. F., Gois, G., Correia Filho, W. L. F., Lima, M., Santiago, B., Freitas, W. K., Santos, P. J., & Costa, M. S. (2020). Fire foci related to rainfall and biomes of the state of Mato Grosso do Sul, Brazil. *Agricultural and Forest Meteorology, 282–283*, 107861. https://doi.org/10.1016/j.agrformet.2019.107861.

Paredes-Trejo, F. J., Barbosa, H. A., & Lakshmi Kumar, T. V. (2017). Validating CHIRPS-based satellite precipitation estimates in Northeast Brazil. *Journal of Arid Environments, 139*, 26–40. https://doi.org/10.1016/j.jaridenv.2016.12.009.

Paschalidou, A. K., & Kassomenos, P. A. (2016). What are the most fire-dangerous atmospheric circulations in the Eastern-Mediterranean? Analysis of the synoptic wildfire climatology. *Science of the Total Environment, 539*, 536–545. https://doi.org/10.1016/j.scitotenv.2015.09.039.

Pereira, J. A. V., & Silva, J. B. (2016). Detecção de focos de calor no Estado da Paraíba: um estudo sobre as Queimadas. *Revista Geográfica Acadêmica, 10*, 5–16. https://doi.org/10.18227/1678-7226rga.v10i1.3173.

R Development Core Team. (2017). R: a language and environment for statistical computing. R Foundation for Statistical Computing, Vienna, Austria, http://www.r-project.org, ISBN 3-900051-07-0.

Rasilla, D. F., García-Codron, J. C., Carracedo, V., & Diego, C. (2010). Circulation patterns, wildfire risk and wildfire occurrence at continental Spain. *Physics and Chemistry of the Earth, Parts A/B/C, 35*(9–12), 553–560. https://doi.org/10.1016/j.pce.2009.09.003.

Ribeiro, H. (2008). Queimadas de cana-de-açúcar no Brasil: efeitos à saúde respiratória. *Revista de Saúde Pública, 42*, 370–376.

Rohlf, F. J. (1970). Adaptative hierarchical clustering schemes. *Systematic Zoology, 19*, 58–82. https://doi.org/10.1093/sysbio/19.1.58.

Santiago, D. B., & Gomes, H. B. (2016). Heat islands in the city of Maceió/AL using orbital data from Landsat 5. *Revista Brasileira de Geografia Física, 9*, 793–803. https://doi.org/10.5935/1984-2295.20160053.

Santos Silva, A., Santos Silva, F. H., Santos, G., & Holanda Leite, M. J. (2019). Desmatamento multitemporal no bioma Caatinga no município de Delmiro Gouveia, Alagoas. *Revista Verde de Agroecologia e Desenvolvimento Sustentável, 14*, 654–657.

Silva, D. F. (2017). Aplicação de Análises de Ondaletas para Detecção de Ciclos e Extremos Pluviométricos no Leste do Nordeste do Brasil. *Revista Brasileira de Meteorologia, 32*, 187–198. https://doi.org/10.1590/0102-77863220002.

Silva de Souza, L., Landau, L., Moraes, N. O., & Pimentel, L. C. G. (2012). Air quality photochemical study over Amazonia Area, Brazil. *International Journal of Environment and Pollution, 48*, 194–202. https://doi.org/10.1504/IJEP.2012.049666.

Silva Lopes, D. V., Silva, D. E., Silva, F. M. S., Paraíso, L. A., Soares, T. L., & Souza, M. C. B. (2018). Áreas de Proteção Ambiental (Apa) de Conservação da Bacia do CELMM. *Caderno de Graduação-Ciências Exatas e Tecnológicas-UNIT-ALAGOAS, 4*, 73.

Silva, B. F. P., Fedorova, N., Levit, V., Peresetsky, A., & Brito, B. M. (2011). Sistemas sinóticos associados às precipitações intensas no Estado de Alagoas. *Revista Brasileira de Meteorologia, 26*, 323–338.

Sokol, R. A., & Rohlf, F. J. (1962). The comparison of dendograms by objective methods. *Taxon., 11*, 33–40. https://doi.org/10.2307/1217208.

Souza, E. B., Kayano, M. T., & Ambrizzi, T. (2005). Intraseasonal and submonthly variability over the Eastern Amazon and Northeast Brazil during the autumn rainy season. *Theoretical and Applied Climatology, 81*, 177–191. https://doi.org/10.1007/s00704-004-0081-4.

Stephenson, D. B., Diaz, H. F., & Murnane, R. J. (2008). Definition, diagnosis, and origin of extreme weather and climate events. *Climate Extremes and Society, 340*, 11–23.

Trenberth, K. E., Fasullo, J. T., & Shepherd, T. G. (2015). Attribution of climate extreme events. *Nature Climate Change, 5*, 725–730. https://doi.org/10.1038/nclimate2657.

Valentin, J. L. (2000). *Ecologia Numérica – Uma Introdução à Análise Multivariada de Dados Ecológicos*. Rio de Janeiro: Interciência.

Ward, J. H. (1963). Hierarchical grouping to optimize an objective function. *Journal of the American Statistical Association, 58*, 236–244. https://doi.org/10.1080/01621459.1963.10500845.

White, B. L. A., & White, L. A. S. (2017). Queimadas e incêndios florestais no estado de Sergipe, Brasil, entre 1999 e 2015. *Floresta, 46*, 561–570.

Zeri, M., Carvalho, V. S. B., Cunha-Zeri, G., Oliveira-Júnior, J. F., Lyra, G. B., & Freitas, E. D. (2016). Assessment of the variability of pollutants concentration over the metropolitan area of São Paulo, Brazil, using the wavelet transform. *Atmospheric Science Letters, 17*, 87–95. https://doi.org/10.1002/asl.618.

Publisher's note Springer Nature remains neutral with regard to jurisdictional claims in published maps and institutional affiliations.